

NORTH AMERICAN PLATE STRESS MODELING:
A FINITE ELEMENT ANALYSIS

by
Lynn Marie Reding

A Thesis Submitted to the Faculty of the
DEPARTMENT OF GEOSCIENCES
In Partial Fulfillment of the Requirements
For the Degree of
MASTER OF SCIENCE
In the Graduate College
THE UNIVERSITY OF ARIZONA

1 9 8 4

STATEMENT BY AUTHOR

This thesis has been submitted in partial fulfillment of requirements for an advanced degree at The University of Arizona and is deposited in the University Library to be made available to borrowers under rules of the Library.

Brief quotations from this thesis are allowable without special permission, provided that accurate acknowledgment of source is made. Requests for permission for extended quotations from or reproduction of this manuscript in whole or in part may be granted by the head of the major department or the Dean of the Graduate School when in his or her judgment the proposed use of the material is in the interests of scholarship. In all other instances, however, permission must be obtained from the author.

SIGNED:

Lynne Marie Reding

APPROVAL BY THESIS DIRECTOR

This thesis has been approved on the date shown below:

Randall M. Richardson

R. M. RICHARDSON
Associate Professor of Geosciences

27 June 1984

Date

ACKNOWLEDGMENTS

I express my sincere gratitude to the one person aside from myself who made this thesis possible, Dr. R. M. Richardson. His enthusiasm for the thesis topic and his inspiration and motivation were a major driving force throughout the duration of my research. I also thank the other members of my thesis committee, Drs. R. F. Butler and Terry Wallace, for laboring through my thesis and providing helpful comments. The research was supported by the NASA grant NAG-5-326.

To Billie Cox, thanks for starting me on the path to the wonderfully esoteric world of finite-element stress modeling and also for the moral support during those pre-talk rehearsal and other more personal trying times. And, of course, I must give thanks to the most witty and clever NEWT I have ever known; his programming assistance with the nefarious HYPER program was invaluable.

But seriously, if it was not for the love, support, and reassurance of my parents, I would never have survived this educational experience.

TABLE OF CONTENTS

	Page
LIST OF ILLUSTRATIONS	vi
LIST OF TABLES	viii
ABSTRACT	ix
1. INTRODUCTION	1
2. DESCRIPTION OF THE NORTH AMERICAN PLATE	6
3. INTRAPLATE STRESS DATA AND PROVINCES	11
Stress Indicators	11
Stress Provinces	13
Mid-Continent Stress Province	16
Atlantic Coast Stress Province	17
Gulf Coast Stress Province	18
Oceanic Stress Province	19
Northeastern Stress Province	20
San Andreas Stress Province	21
Basin and Range Stress Province	22
Colorado Plateau Stress Province	23
Southern Great Plains Stress Province	24
Pacific Northwest Stress Province	24
Alaska Stress Province	24
4. MODELING METHOD	26
Elastic Models	30
5. POTENTIAL PLATE DRIVING FORCES	32
Ridge Forces	32
Line Ridge Forces	34
Distributed Ridge Forces	38
Gravitational Sliding Formulation	38
Cooling Half-space Formulation	40
Ridge Force Test Case	43
Continental Topography Forces	49
Continental Topography Force Test Case	56
Continental Topography Related to the Geoid	62
Transform Boundary Forces	65
Caribbean Transform Boundary	66

TABLE OF CONTENTS--Continued

	Page
San Andreas Transform Fault	69
Normal Forces	70
Convergence Forces at Subduction Zones	71
Aleutian Convergence Forces	72
Cocos Convergence Forces	73
Drag Forces	73
Driving Drag	74
Resistive Drag	75
Variable Drag	76
6. MODELING RESULTS	77
Ridge Models	77
Line Ridge Model	77
Coarse-grid Distributed Ridge Model	80
Fine-grid Distributed Ridge Model	85
Driving-drag Model	86
Pacific Boundary Model	88
Southern Boundary Model	92
Continental Topography Model	95
7. DISCUSSION AND CONCLUSIONS	101
REFERENCES	107

LIST OF ILLUSTRATIONS

Figure		Page
1.	Tectonic plates on a Mercator projection	7
2.	North American plate on a Lambert projection	8
3.	Finite-element grids	14
4.	North American plate stress provinces and dominant stress trends.	15
5.	Line ridge forces	37
6.	Distributed ridge forces	41
7.	Test grids	45
8.	Total cumulative forces and stresses from ridge force test case	47
9.	Contoured crustal thicknesses for North American plate . .	53
10.	Three-dimensional topography of the North American plate on a Mercator projection	54
11.	Schematic of the density moment for an oceanic column . .	58
12.	Continental topography forces based on density moments. .	61
13.	Geoid undulations referred to the hydrostatic flattening of $1/299.638$	64
14.	Boundary forces for the North American plate	67
15.	Resulting stresses from ridge force models	81
16.	Force model DRD1 and resulting stresses	83
17.	Force model DRD2 and resulting stresses.	84
18.	Force model DRD3 and resulting stresses	87
19.	Force model DD and resulting stresses.	89
20.	Force model DP and resulting stresses.	91

LIST OF ILLUSTRATIONS--Continued

Figure		Page
21.	Force model DPS and resulting stresses	94
22.	Force model DPSN and resulting stresses	96
23.	Force model TD and resulting stresses.	98
24.	Resulting stresses from force model BT	99
25.	Model BT forces.	100

LIST OF TABLES

Table		Page
1.	Description of force models	78
2.	Torque parameters for force models	79

ABSTRACT

An elastic finite-element analysis of the North American plate provides a method for calculating intraplate deformation in response to various tectonic forces. Forces considered in the modeling include line ridge, distributed ridge, transform, convergence, and basal drag. In situ stress, earthquake, and structural data constrain the modeling scheme. An initial grid with 328 planar triangular elements and 190 nodes and a finer grid with 718 elements and 396 nodes were tested. Resistive basal drag was used to balance net torque on the plate due to boundary forces. Calculated stress for ridge-force and driving-drag models agree with the observed stress orientations in the stable continental interior of the plate. Additional forces applied to other plate boundaries of the ridge models yielded a better fit to observed stresses near the plate boundaries. Modeling results suggested that ridge forces are probably the dominant mechanism for driving and stressing the North American plate.

CHAPTER 1

INTRODUCTION

The Earth's lithosphere is composed of approximately 12 major plates, which simplistically can be thought of as rigid caps moving with respect to each other on the surface of a sphere. Plate tectonics is the science that deals with the causes and effects of this motion. Most deformation of the lithosphere is due to tectonic processes and occurs along plate boundaries; in fact, these anomalously high deformational regimes, as evidenced by seismicity, are defined as the boundaries. Deformation within the interior of the plates also occurs and can be related to certain tectonic processes that affect the interplate stress regime. The presence of diffuse seismicity patterns in the interior regions of the plates suggests that the plates are in fact not rigid bodies but should possibly be considered as deformable bodies. The relationship between intraplate deformation and tectonic processes acting along plate boundaries is not well understood. The major objective of this thesis was to investigate the effects of potential plate-driving mechanisms on intraplate stresses for the North American plate.

A finite-element technique was used to model the response of the North American plate to various potential plate-driving forces that act along the plate's boundaries. Various geometric and rheologic properties for the plate were incorporated into the models. These properties control the response of the plate to various tectonic loading

schemes. Boundary conditions or certain plate motion constraints also influence intraplate response to applied loads.

The basic procedure used in the modeling scheme is as follows. The North American plate was divided into a finite number of triangular elements. Two grids with 328 and 718 elements and 190 and 396 node points, respectively, were used. Structural properties such as crustal thickness, topography, bathymetry, and elemental area as well as rheologic properties such as Young's modulus, Poisson's ratio, and density contrasts were all incorporated into the problem as known values. The plate was treated as an elastic medium. Potential driving and resistive tectonic forces, which act along certain boundaries or on the base of the plate, were applied along boundary nodes or to the base of the plate. The direction of these forces was based on reasonable approximations of relative plate motion vectors and other data. Almost all of the intraplate stress data available to constrain the modeling consisted of the orientations of principal stresses. Very little information exists on the magnitudes of tectonic stresses in the plates, and thus it was difficult to constrain the absolute magnitudes of potential forces acting on the plates. Some potential forces are reasonably well constrained in magnitude, particularly ridge forces, but many are subject to large uncertainties in magnitude and even occasionally in sign. Thus, most of the models considered will assume a reasonable value for ridge forces and attempt to constrain the relative contribution of other forces. Different boundary conditions and torque-balancing forces were tested so that the plate remains in mechanical equilibrium. A combination of boundary and basal forces was sought by comparing predicted stresses

from each model with the actual observed intraplate stress states and improvements to the models were made such that a best-fit stress solution for the whole plate was obtained. In addition to tectonic forces, topographic forces in the continental interior of the plate were added to the modeling scheme in hopes of being able to predict any localized intraplate stress features due to lateral density contrasts.

The stress data base used to constrain the predicted stresses was an extensive collection of inferred principal stress orientations based on earthquake focal mechanisms, in situ stress measurements, and geologic features. The plate was divided into a number of stress provinces, each of which is associated with a dominant, characteristic stress patterns of either tectonic or local origin. Initial modeling was conducted in an attempt to match the dominant east-northeast maximum compressive stress trend inferred for the stable continental interior of the plate.

The potential driving forces considered in the models included ridge forces, shear tractions and normal forces along transform boundaries, boundaries forces at subduction zones, and driving and resistive basal drag forces. Three different parameterizations or formulations were used to model ridge forces. Line ridge forces were applied along the ridge crest and distributed ridge forces were applied throughout the young oceanic lithosphere by using both a gravitational sliding and a cooling half-space formulation.

The modeling schemes presented in this thesis are an extension of global finite-element modeling done by Richardson (1979b). Advances to this preliminary modeling include single-plate modeling of the

North American plate. Distributed ridge forces were also used as a more accurate representation of the ridge force than the line ridge approximation previously used. Topography-related forces are also a new addition.

A geographic description of the plate will be presented as well as a description of the stress provinces and stress data available for each province in the plate. The modeling method will be described, including specifics on grid dimensions and elastic parameters. Each type of force will be discussed in detail. Numerous test cases will be presented that were conducted to compare modeling results from the different ridge force formulations with each other and with analytic solutions. The validity of the formulation used to model forces related to continental topography was also investigated in test cases.

Finally, all significant force models and their resulting intraplate stresses will be presented and discussed, starting with the initial oversimplified line ridge models that were run in hopes of fitting the dominant mid-plate stress trend. Increasingly complicated models, which realistically represent the tectonic processes occurring along all boundaries, along the base of the plate, and within the continental portions of the plate, will be presented. Basically, improvements to fitting the intraplate stress data were progressively made with improvements to the models until what is believed to be the best possible fit to the data as allowed by a modeling scheme of this nature was achieved. Conclusions drawn about the significance and influence of certain tectonic processes on the intraplate stress regime of the North American plate

will be discussed as well as the limitations of the modeling scheme and possible explanations for some of the calculated results.

CHAPTER 2

DESCRIPTION OF THE NORTH AMERICAN PLATE

The North American plate is a relatively large section of lithosphere with a variety of different boundary types and a unique motion in the hot-spot reference frame. Figure 1 reveals in a Mercator projection the location of this plate with respect to surrounding plates. The plate is chiefly composed of continental lithosphere ; however, a substantial portion of oceanic lithosphere exists. Figure 2 is an illustration of the plate boundary on an equal-area Lambert projection; this projection was used to display modeling results so that large area distortions near the geographic pole were eliminated. The boundary of the North American plate is defined by seismicity; however, almost no seismic activity is recorded that would justifiably define a boundary between the North and South American plates. It is the different relative rotations of the African plate with respect to the two American plates (Chase, 1977; Minster and Jordan 1978) that requires that these two plates be treated as separate entities. The boundary between the American plates is believed by some (e.g., Funnel and Smith, 1968; Ball and Harrison, 1970) to be located near the Barracuda Ridge, along a left-lateral shear zone, due to its observed characteristic fracture zone features. Seismic activity northeast of the ridge in the Barracuda abyssal plain may supply further evidence for the tectonic significance of this region. For modeling purposes, a boundary between these two

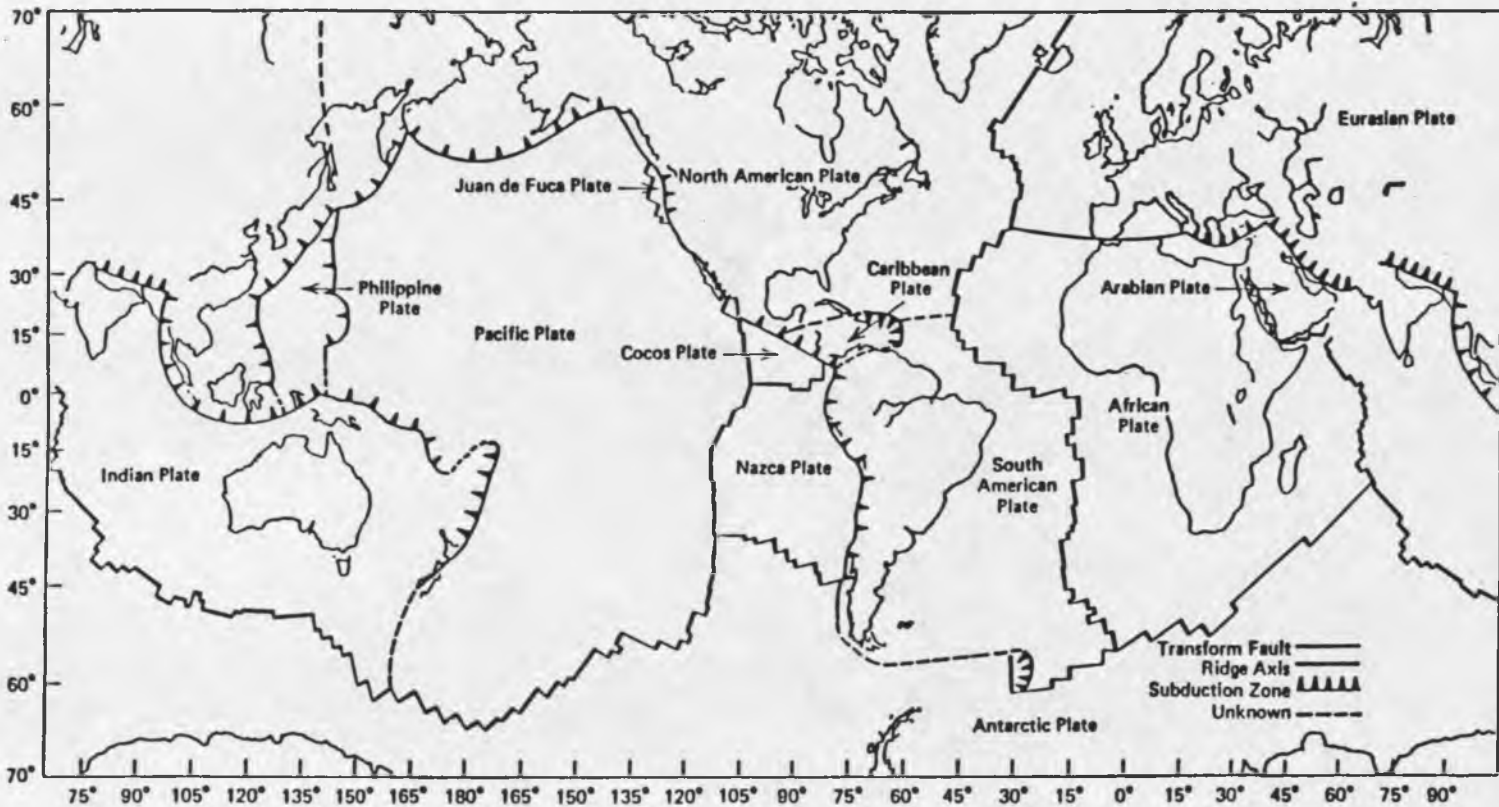


Figure 1. Tectonic plates on a Mercator projection. -- From Turcotte and Schubert (1982)

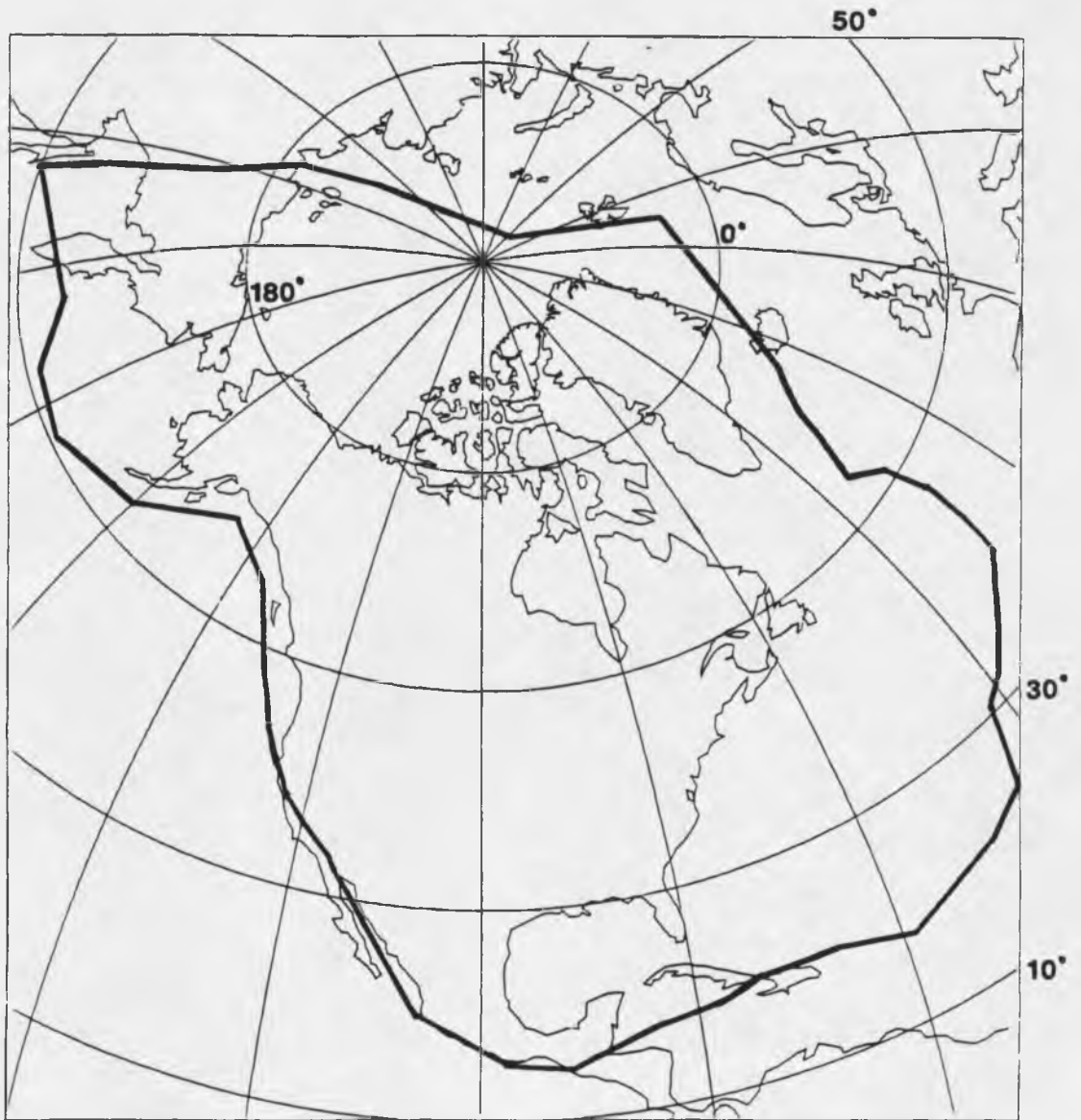


Figure 2. North American plate on a Lambert projection

plates was taken from the Lesser Antilles at approximately lat 18° N. to the African plate such that the boundary includes the 23 Oct. 1964 strike-slip earthquake, which occurred at approximately lat 20° N., long 56° W. From the junction of the American plates with the African plate, the Mid-Atlantic Ridge extends northward as the eastern boundary of the North American plate. This spreading center continues through Iceland, over the north geographic pole, and finally dies out in the Arctic Ocean as it approaches the continental shelf of Siberia. From this point, it is uncertain where the boundary meets the Pacific plate, but a commonly accepted trend for the boundary between the North American and Eurasian plates as it approaches the Pacific plate is shown in Figure 1 (Chase, 1977). The junction between these three plates is taken near Sakhalin, slightly northwest of the Kuril Trench. From this point the boundary continues eastward past the Kamchatka Peninsula at which point the Aleutian Trench begins to mark the boundary where the Pacific plate is subducting beneath the north American plate. Along a short segment of the western boundary of the North American plate, south of Alaska, the Juan de Fuca plate is subducting beneath the North American. Also along the western boundary, the San Andreas transform fault extends from the Middle American Trench near the southern end of Baja California northward to the Mendocino fracture zone north of San Francisco. Along the Middle American Trench, the Cocos plate subducts beneath Central America. Finally, south of the Yucatan Peninsula, the transform boundary along the Cayman Trough of the Caribbean plate begins and continues to the Puerto Rico Trench. The small segment of the Caribbean boundary between

Puerto Rico and the Lesser Antilles under which the North American plate is being subducted is the only location at which subduction of the North American plate occurs beneath another plate.

The internal morphology of the plate is quite complex. There are essentially three types of lithosphere for the plate: oceanic, continental shelf, and continental. Each type has unique elastic properties associated with it. All continental and shelf lithosphere was assumed to have a thickness of 1×10^5 m, whereas the oceanic lithosphere was assumed to be 5×10^4 m thick. Within each of these different lithospheric types, especially the continental, there are a variety of terrains and regions with varying rheologic properties, topographic and geologic features, and lateral density contrasts. Hence, certain assumptions and generalization used in a modeling scheme for a certain type of lithosphere may not apply to work well for all regions within the plate. Certain regional provinces within the plates, defined by their unique stress patterns, will be discussed in the next chapter.

CHAPTER 3

INTRAPLATE STRESS DATA AND PROVINCES

Intraplate stresses are the result of the tectonic processes that act along plate boundaries and the internal plate mechanisms that influence stress trends on a local scale. Delineation of regional versus local stress trends is essential to be able to evaluate the tectonic forces that influence the intraplate stress field. In general, tectonic stresses have a more coherent, consistent, and broad-scale pattern than local phenomena. Dominant stress provinces and stress indicator techniques for the North American plate will be discussed.

Stress Indicators

Seismicity is probably the best indicator of active intraplate deformation (Zoback and Zoback, 1980). Fault-plane solutions provide information about principal stress orientations at a seismic source; they sample stress over a greater volume of lithosphere and depth over a great range than other in situ stress indicators. Inherent uncertainties associated with inferred stress orientations from a single fault-plane solution exist. However, these uncertainties are minimized if a number of consistent fault-plane solutions can be used to infer a characteristic pattern of stress orientations for a region. However, stress orientations inferred from fault-plane solutions may not uniquely represent the state of stress throughout the entire thickness of the lithosphere

because most intraplate earthquakes occur at relatively shallow depths in the lithosphere.

There are two in situ methods that may be used to estimate stress: strain relief, or overcoring, and hydrofracturing. The strain-relief technique is based on the relaxation response of a surface after a stress has been removed. After the elastic parameters of a sample have been determined in the laboratory, Hooke's law can be used to calculate stresses from measured strains. In the hydrofracture technique, stresses are measured directly by applying pressure to a closed borehole section until the borehole fails (Zoback, Tsukahara, and Hickman, 1980).

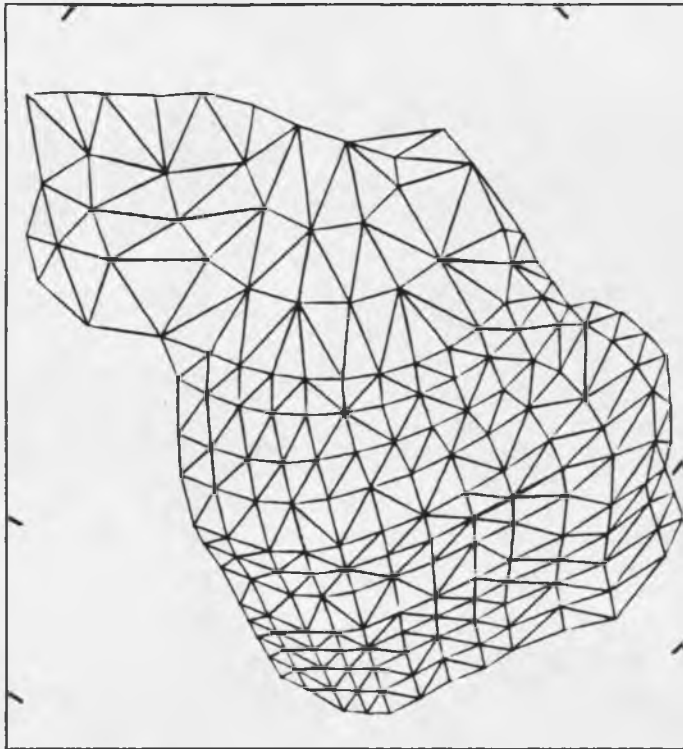
Large geologic features may provide additional information on principal stress orientations. For example, inferences about stress fields may be made from horizontal slip directions on faults. Linear volcanic structures usually lie along planes perpendicular to axes of least principal stress and hence are another type of geologic stress indicators (Nakamura, Jacob, and Davies, 1978). The trends or orientations of postglacial buckled structures can also be used to infer perpendicular directions to maximum compressive stress trends (Sbar and Sykes, 1983).

Interpretations of stress data based on these measurement techniques depend on the technique(s) used and the consistency in the data. Several other factors such as residual strains, loading histories, thermally induced stresses, and effects of local topography may affect regional stress patterns or completely overmask regional trends.

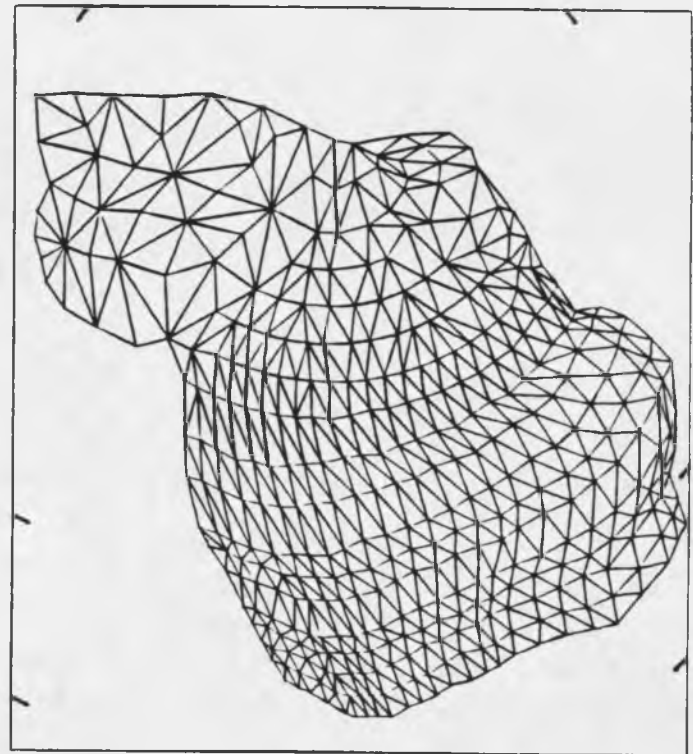
Stress Provinces

Intraplate deformation generally occurs at a lower rate and in a more sporadic fashion than interplate deformation. Within the interior of the North American plate, a stress province can be defined as a coherent pattern of stress orientations. Node spacing of the coarse grid (Figure 3) constrains the amount of resolution attainable in calculating intraplate stresses. Because the distance between nodes ranges from a few hundred to a thousand kilometers, stress provinces are defined such that they encompass a significant number of elements. Some of these large-scale provinces are defined by characteristic regional stress trends due to the tectonic processes driving the plate; other provinces represent stress states that are possibly related to these tectonic processes but are probably influenced to a greater degree by local or remanent phenomena. Specific stress provinces of the plate were specified and individually investigated in terms of the processes that attribute to their characteristic stress states. These provinces are outlined in Figure 4.

The abundance of intraplate stress data for continental North America is overwhelming. The sources of these data are quite numerous. Thorough compilations of such data are included in a few sources: Zoback and Zoback (1980), Zoback and others (n.d.), and Richardson (1987b). By using data from these sources, large-scale characteristic stress regions were established for the North American plate. A description of characteristic stress trends and the data used to define these trends will be discussed for each province.



a. Coarse grid with 328 elements
and 190 nodes



b. Fine grid with 718 elements
and 396 nodes

Figure 3. Finite-element grids

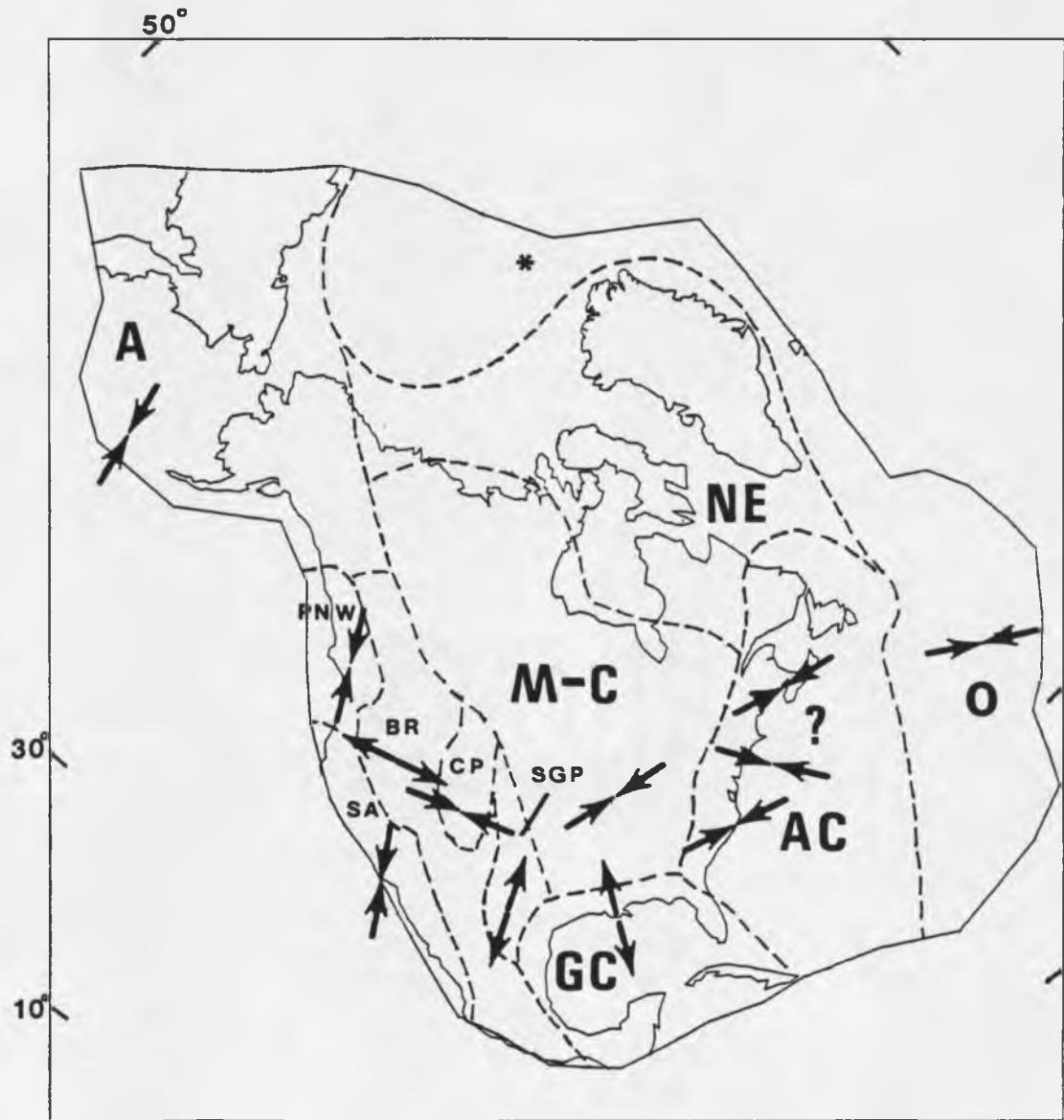


Figure 4. North American plate stress provinces and dominant stress trends

Mid-Continent Stress Province

The Mid-Continent stress province in the stable continental interior is the largest area of the North American plate for which a relatively consistent trend for principal stresses exists. This stress province encompasses the central and eastern portions of North America east of the Rocky Mountains, north of the Gulf Coastal Plain, and west of the Appalachian fold belt. The province includes the western Canadian basin and the Canadian Shield north to the Arctic coast. Characteristic maximum horizontal compressive principal stresses in this tectonically stable region trend northeast to east-northeast. The uniformity of this stress pattern over such a large area suggests that these inferred stresses are probably of tectonic origin.

Fault-plane solutions for this province typically indicate strike slip and thrust or reverse movement along fault planes. Deviations from this trend, e.g., in the New Madrid area in southeastern Missouri, are assumed to be the result of localized effects and are not indicative of lithospheric response to tectonic processes.

Consistent with the focal mechanism solutions, stresses inferred from in situ measurements provide valuable information in seismically inactive areas. Numerous hydrofracture and strain-relief measurements were taken in the mid-continent region of North America. References and descriptions of these measurements were taken from Zoback and Zoback (1980) and Richardson (1978b). Sbar and Sykes (1973) found geologic features such as post-glacial buckles and pop-ups that trend northwest. The trends of these features suggest that maximum compressive stress orientations should be northeast.

In situ work done by Gough, Fordjor and Bell (1983) and Fordjor, Bell and Gough (1983) suggest that this stable continental interior province extends to the Arctic coast through the western Canadian sedimentary basin. They used alignment of fractures or "break-outs" in oil wells to infer horizontal compressive stress orientations in this region.

Atlantic Coast Stress Province

Zoback and Zoback (1980) defined their Atlantic Coast stress province as that region including the Atlantic Coastal Plain, the Piedmont province of the southern Appalachians, and all of the Appalachian fold belt in the northeast. Early investigations by Sbar and Sykes (1983) revealed their stress states in the Atlantic coastal region are consistent with the stable continental interior. Recent studies in South Carolina indicated that stress trends in the southern Appalachians may be consistent with those in the stable continental interior (e.g., Talwani, 1981; M. L. Zoback, 1984, personal commun.) The most recent stress indicator near Auburn, New York, is a hydrofracture measurement in a 1.6-km deep well (Hickman, Healy, and Zoback, n.d.). From orientations of hydraulic fractures at 593-m and 919-m depths, maximum horizontal principal stress azimuths are inferred to be N. $82^{\circ} \pm 15^{\circ}$ E. However, Zoback and Zoback (1980) and Zoback and others (n.d.) have compiled a wealth of stress data that suggest that maximum horizontal compressive stresses in this region trend northwest. The evidence for this trend in the southern portion of the Atlantic Coast is not as convincing and overwhelming as the abundant data

north of lat 40° N. The orientations inferred for the southern region by Zoback and Zoback (1980) are based primarily on fault offsets in post-Eocene sediments. Numerous in situ measurements as well as focal mechanisms have been gathered for the northern Atlantic coastal region. Fault-plane solutions suggest that earthquakes in this region are usually characterized as thrust and strike-slip motion along their fault planes. The orientations of the fault planes suggest compression perpendicular to the coastal margin in a northwest direction.

Stress trends in this province are most recently believed by M. L. Zoback (1984, personal commun.) to be consistent with the Mid-Continent stress province in the southern Appalachians up to lat 37° N. and along the northeastern seaboard above Maine. However, she believes that maximum principal stress orientations in the northern Appalachians south of Maine and east of the Adirondacks and the Auburn well trend northwest.

The continental shelf of North America is also included in this stress province. Continental shelves mark the boundary between continental and oceanic lithosphere. These passive margins are unlike plate boundaries in that they lack abundant seismic activity. However, stresses associated with the subsidence of sedimentary material and lateral density inhomogeneities along the shelf may exist.

Gulf Coast Stress Province

The Gulf Coast stress province includes the southern portion of the Gulf Coastal states and extends into the Gulf of Mexico. Within this region, a sediment-loading phenomenon appears to be the dominant

process affecting the stress states. Throughout the province, the greatest principal stress is in the vertical direction; the least principal stress is oriented perpendicular to the continental margin (Zoback and others, 1978), thus suggesting that an extensional stress regime characterized by normal faulting exists for this province. The stress data used by Zoback and Zoback (1980) to infer stress orientations include orientations of recently active faults and Late Tertiary normal faults. Other in situ indicators are restricted to the shallow sediment layers and do not sample the underlying bedrock, hence they reveal stress conditions for local, shallow phenomena and not regional tectonic processes.

One well-recorded earthquake occurred in the Gulf of Mexico in 1978. A focal mechanism for the event indicates north-south compression instead of tension as inferred from earlier studies of fault planes in that region (Frohlich, 1982); however, the magnitude of this earthquake is probably too small to indicate anything about the regional stress regime.

Oceanic Stress Province

Both continental and oceanic types of lithosphere exist for the North American plate. The continental margin is represented by the offshore shelf, which is included in the coastal provinces for the purpose of this investigation. The Oceanic stress province includes all oceanic lithosphere less than approximately 100 m.y. old in the North Atlantic and Arctic Oceans. The oceanic material is less susceptible to focal phenomena such as glacial buckling and sediment loading. At

present, investigators of the Oceanic stress province are limited to earthquake focal mechanisms, although oceanic wellbore breakout data from the Pacific plate (Newmark, Zoback, and Anderson, 1984) indicate that other techniques may soon be available for inferring stress in an oceanic plate. With the possible exception of thermally induced stresses caused by cooling of the oceanic lithosphere, oceanic stresses in the North American plate are probably related to tectonic processes occurring at the Mid-Atlantic Ridge. Maximum horizontal compressive stresses are oriented approximately parallel to downdip or increasing-age directions from the ridge. The magnitudes of these compressive stresses due to forces from the elevated ridge are analytically determined to be on the order of several tens of MPa (e.g., Lister, 1975; Richardson, Solomon, and Sleep, 1979; Turcotte and Schubert, 1982; Fleitout and Froidevaux, 1983). Localized normal faulting events near the ridge crest are probably the result of local effects related to the upwelling of mantle material at the spreading axis. Another local effect that may dominate tectonic stresses occurs along the Reykjanes Ridge in Iceland. Haimson and Voight (1977) claimed that thermoelastic processes caused maximum horizontal compressive stress orientations to be oriented parallel instead of perpendicular to the ridge in Iceland.

Northeastern Stress Province

The Northeastern stress province encompasses the northernmost part of North America, the Baffin Bay, and the Labrador Sea, and it extends over to Greenland. The greatest concentration of data for this province lie in the Baffin Bay area. Zoback and others (n.d.) are

presenting extensive focal mechanism data throughout the region. From their compilation they determined that a wide range of stress states appears to exist for this province. They also indicated the wide variety of local processes that could possibly contribute to the range of observed stress orientations and deformational styles. Some of these mechanisms are believed to be related to preexisting faults and fracture zones and sedimentary loading phenomena along continental shelves. The data are quite diffuse in this province, and no characteristic trend can be inferred from the data base. With the inclusions of this province, all regions in the eastern portion of the North American plate (east of the Rocky Mountains) have been defined or incorporated into some stress province.

San Andreas Stress Province

East and west of the Rocky Mountains lie two seemingly independent tectonic regimes. Tectonic processes that appear to be affecting the western region are probably the result of Pacific and North American plate interactions. The San Andreas transform boundary between these two plates is the most seismically active region in the North American plate and is thus being considered as an individual province—the same province as defined by Zoback and Zoback (1980). The major fault trends northwest with conjugate faults striking at angles oblique to this trend. The orientation of the maximum horizontal compressive stresses are approximately north-south (Zoback and Zoback, 1980). The general style of deformation is strike slip, thus the least principal stresses are characterized by deviatoric tension in an

east-west direction. This style of deformation changes near the Big Bend region of the San Andreas fault. Here thrust and reverse faulting predominate, thus stress in the vertical direction is the least principal stress. Near the Big Bend area, compressional features sub-parallel to the fault suggest that a normal component of compression exists along the fault (Zoback and others, 1978).

The Garlock fault, south of the Big Bend, is included in the San Andreas stress province. This left-lateral fault extends eastward to the boundary of the Basin and Range stress province. North of the Garlock fault, the Sierra Nevada Range marks a transitional zone in which the chiefly strike-slip deformational style observed in the San Andreas stress province changes to an extensional tectonic regime in the Basin and Range stress province.

Basin and Range Stress Province

The Basin and Range stress province is bounded by the Sierra Nevada in the west and the Intermountain Seismic Belt in central Utah and Arizona to the east. It extends north into Oregon and south in Central America to the Cocos boundary. The stress pattern observed in the Rio Grande Rift in New Mexico and Colorado is similar to that in the Basin and Range stress province, so this area to the east of the Colorado Plateau is included in the Basin and Range stress province.

The Basin and Range stress province is characterized by a relatively thin crust, high heat flow, and regional uplift and extension (Stewart, 1977; Zoback and others, n.d.). Normal and strike-slip faulting is the characteristic deformation style inferred for this region.

Deviatoric tensional stresses are generally oriented west-northwest. Components of strike-slip motion on the normal faults are observed in the southern portion of the province (Zoback and Zoback, 1980). These stress orientations are constrained by numerous focal mechanisms determined for this region. Little or no seismic data exist for Mexico, so northern Mexico is included in this province simply due to lack of evidence to claim it an individual stress province. Perpendicular compressive stresses related to the subduction of the Cocos plate beneath Mexico may occur landward from this boundary. The northern Rocky Mountains are also included in this province because stress states in this region are consistent with those in the Basin and Range stress province. Smaller stress provinces in between these two areas, e.g., the Snake River plain, are assumed to be due to very localized phenomena and are not indicative of regional processes. Also areas of this small size are not within the resolution of the models.

Colorado Plateau Stress Province

The Colorado Plateau stress province is most easily described as the interior of the Colorado Plateau, excluding a few hundred kilometers on both sides of the physiographic province and including the Wyoming Basin and portions of the Southern and Middle Rocky Mountain physiographic provinces. A 90-degree rotation of least principal stress axes occurs in this province from the Basin and Range stress province. Seismicity in the province is rare, except in the northern portion of the plateau. The absence of substantial seismic activity may suggest relatively small differential stresses (Zoback and Zoback, 1980). Horizontal

compressive stresses are generally oriented west-northwest. Both strike-slip and thrust faulting occurs in the province.

Southern Great Plains Stress Province

The Southern Great Plains stress province includes north-central Texas, eastern New Mexico, and Colorado. The region is a uniform transitional zone between the extensional tectonic regimes to the west and the compressive tectonics observed to the east. Numerous references of geologic and in situ stress indicators as well as focal mechanisms for this province are cited by Zoback and Zoback (1980). Most of these indicators reveal normal faulting events throughout the region. The least principal horizontal stresses are oriented approximately north-northeast.

Pacific Northwest Stress Province

The area included in the Pacific Northwest stress province is slightly larger than the Pacific Northwest stress province of Zoback and Zoback (1980). It includes most of Oregon, Washington, and southern British Columbia. The greatest horizontal principal stress direction is consistent with orientations of this stress component in the San Andreas stress province. Both strike-slip and thrust faulting occurs as a result of north-south compression in the region. These conclusions are drawn from numerous focal mechanisms given by Zoback and Zoback (1980).

Alaska Stress Province

With the exception of Alaska and the Aleutian arc complex, stress data in the northwestern portion of the North American plate is

nonexistent. This region of the plate, including Alaska, the Bering Sea, and the northwest corner of Asia, will be considered the Alaska stress province. Numerous geologic and volcanic, in situ "breakouts," and seismic stress indicators exist for the Bering Sea and Alaska. Most data consistently reveal maximum horizontal compressive stress orientations in an approximately northwest direction (Nakamura and others, 1977; Jacob and Perez, 1982). These orientations are approximately subparallel to the relative motion vectors between the Pacific and North American plates.

CHAPTER 4

MODELING METHOD

In using a finite-element technique to model the North American plate, the plate is treated as a linearly elastic continuum. The displacement method of finite elements is used in the modeling scheme. The fundamental constraint in the modeling is that the elastic plate remain in mechanical equilibrium. Hence, all external loads applied to the plate must be balanced by internal strains. In the displacement method, the continuous medium is divided into a number of triangular elements of finite area. These elements are interconnected by a finite number of points called nodes. When external loads are applied to the medium of known rheologic and geometric properties, unknown displacement of the internal node points may be calculated. Displacement within an elemental area may be evaluated from nodal point displacements. The number of nodes per element determines the order of the polynomial functions that uniquely define the displacement within an element in terms of the elements nodal displacements. Because displacements within the triangular elements vary linearly in x and y , the strain within a given element is independent of location within the element and has a constant value. The dimension of the matrix containing the polynomial functions is determined by the degree of freedom or coordinate directions of displacement for any interior point of an element. The triangular elements used to model the North American plate have two

degrees of freedom at each node point: one in the latitudinal and one in the longitudinal direction. The total degrees of freedom per element is therefore six. The degrees of freedom for any interior point of an element are a function of the corresponding nodal degrees of freedom for the element. Rigid-body motion is constrained by "pinning" specific node points. By pinning a node, certain degrees of freedom for that node are constrained.

The relationships between displacement within an element i and the elemental strain is given by:

$$\{\epsilon\} = [B_i] \{\delta\}^e$$

where: $\{\epsilon\}$ = strain vector

$\{\delta\}$ = nodal displacement vector

$[B_i]$ = strain operator matrix containing derivative operators of the nodal displacements.

The displacement functions define the strain within an element which, in turn, determines the state of stress throughout and along the boundaries of an element. The elastic relationships between stress and strain is linear and is given by:

$$\{\sigma\} = [D_i] \{\epsilon\}$$

where: $\{\sigma\}$ = element stress vectors

$[D_i]$ = elasticity matrix that contains certain material properties.

From stress-strain relationships given by Hooke's law for plane stress, the elasticity matrix is given in the form:

$$[D_i] = \frac{E}{1 - \nu^2} \begin{bmatrix} 1 & \nu & 0 \\ \nu & 1 & 0 \\ 0 & 0 & \frac{1-\nu}{2} \end{bmatrix}$$

where: E = Young's modulus

ν = Poisson's ratio.

An element stiffness matrix dependent on the geometry and the elastic properties of the element is then calculated from the relation (Zienkiewicz, 1971):

$$[K_i] = \int_{\text{Area}} [B_i]^T [D_i] [B_i] h \, dx \, dy$$

where: h = thickness of element.

Each elemental stiffness matrix in a local coordinate system is transformed to a global stiffness matrix [K] representing the entire plate. In addition, a global matrix [U] is established as the vector of unknown nodal displacements for the whole plate. The matrix [F] is defined as a vector that contains all equivalent nodal force information in the global coordinate system. The term "equivalent nodal force" refers to the static equivalence of the nodal loads to the boundary stresses and the distributed loads (acting on a unit volume within an element in the same direction as the displacements of the volume) on the element (Zienkiewicz, 1971). These three matrices are used to establish the equilibrium condition for a finite-element approximation to an elastic medium given by Bathe and Wilson (1976):

$$[K] [U] = [F] \quad (4-1)$$

Evaluating this expression involves making reasonable assumptions for [F], providing the information necessary to develop [K], and through inverse techniques solving for [U].

Solving finite-element problems entails multiple matrix operations on relatively large linear systems. Efficiency in developing the problem is essential for time and economic reasons. It is thus advantageous to use constant-strain triangular elements to model the plate. Higher order elements would increase the number of degrees of freedom and hence drastically increase the size of the problem. Also, triangular elements of a plate on the Earth's surface best approximate the sphericity of the Earth.

The coarse grid is composed of 328 elements and 190 nodes, which yields 380 degrees of freedom (Figure 3a). The finer grid has 718 elements and 396 nodes for which there are 792 degrees of freedom (Figure 3b).

The wave-front solution technique of Irons (1970) is used to evaluate the equilibrium condition of equation (4-1). This technique, based on Gaussian elimination, requires the assemblage in in-core storage of a stiffness matrix of elements having a particular degree of freedom. Back substitution coefficients from this matrix are then transferred to external computer storage as this degree of freedom is removed from the problem. The transfer of in-core stiffness matrix elements for a certain degree of freedom to external storage is continued until all degrees of freedom have been removed. Before any one degree of freedom is eliminated, a minimal number must be simultaneously assembled. This number is called the front width of the problem.

Optimizing the element numbering scheme in a problem minimizes this value and increases the central processing unit (CPU) time necessary to perform the calculations.

The front width of the coarse North American grid ranges from 35 to 38, depending on the degrees of freedom specified for a given model; for the fine grid the front width increases to 90. The CPU time necessary to execute program SOLV, which performs the finite-element analysis, increases from about 10 seconds for the coarse grid to 66 seconds for the fine grid on the University of Arizona's CYBER 176 computer.

Once all degrees of freedom have been eliminated, back substitution is used to evaluate the nodal point displacements in an order that is the reverse of the degree of freedom elimination scheme. Once [K] has been constructed, it is left in outside storage in order to minimize compilation time.

Elastic Models

The North American plate is treated as an elastic medium for which oceanic elements are assigned a thickness of 5×10^4 m and continental elements a thickness of 1×10^5 m. A value for Young's modulus used for all lithospheric elements is 7.0×10^{10} N/m²; however only a spatial contrast in the value of E affects calculated stresses because forces rather than displacements are applied. Poisson's ratio, ν , is taken to be 0.25.

The finite-element technique allows for variable elastic parameters and material properties to be used for different elements. A more

realistic way of modeling the relatively warm mantle material at the Mid-Atlantic Ridge would be to use a smaller value for Young's modulus. Likewise, convergent zones and transform faults may act as soft regions as well as some intraplate regions such as the Basin and Range stress province. Variable Young's moduli may be assigned to these regions to better model their rheologic properties. For the purpose of this investigation, however, all models assume a homogeneous elastic medium.

CHAPTER 5

POTENTIAL PLATE DRIVING FORCES

The forces that act on the North American plate can be divided into at least four types: (1) ridge forces related to the gravitational potential of the elevated Mid-Atlantic Ridge, (2) forces that act along shearing or transform boundaries and provide resistance to the relative motion between the North American and adjacent plates, (3) forces that act on the plate across subduction zones, and (4) basal drag forces that act along the bottom of the plate. The basal force types may include driving drag and resistive drag both of which are a function of the relative motion of the lithospheric plate over the less viscous asthenosphere.

Ridge Forces

The Mid-Atlantic Ridge accounts for about two-thirds of the length of the boundary between the North American plate and surrounding plates. Ridge forces thus substantially dominate any other boundary force type in terms of area over which the force acts. This areal dominance suggests a great potential for ridge force to be a major contributing type of force in the mechanical process that drives the North American plate.

The Mid-Atlantic Ridge becomes a topographic feature marking a zone of plate divergence. The ridge is elevated when the upwelling of the hot mantle material increases the buoyancy of the hotter, thinner

plate at the ridge axis. As the plate moves away from the ridge, it cools and thickens and becomes more dense; hence it sinks deeper into the mantle. Lateral density contrasts associated with the spreading plate induce a gravitational potential throughout the length of the plate whereby a component of the gravitational field causes it to spread away from the crest by gravity sliding. The occurrence of the gravitational sliding phenomenon can also be explained as the elevated ridge's having excess potential energy and spreading out in order to obtain a lower energy state (Forsyth and Uyeda, 1975). The ridge force acts along the gradient of steepest slope or in the direction of most rapid age increase from any given point along the ridge crest. By choosing a reasonable value for the force exerted on the surface plate due to gravitational sliding, the importance of lithospheric thickening to the total driving mechanism is determined. Using simple flow models, Hager and O'Connell (1981) showed that thermally induced density contrasts in the lithosphere are sufficient to drive plates a few centimeters a year and stress the interior regions of a plate. Hager and O'Connell also believed that ridge body forces are more important contributors to the total driving mechanism than the net body forces associated with a sinking slab. Previous work done by Artyushkov (1978) and Richardson (1976a) also supported this hypothesis. Lister (1975) and Turcotte and Schubert (1982) believed that the total force due to elevated ridges and the net force from subducting slabs are on the same order of magnitude; without any subducting slab attached to the North American plate, ridge forces appear to have the greatest potential to drive the plate.

The forces acting on the plate due to the elevated ridge may be evaluated by considering the total force balance for the surface plate (Artyushkov, 1973; Lister, 1975; Turcotte and Schubert (1982)). This net horizontal force on the lithosphere is found by subtracting the total force on the upper surface of the lithosphere and the integral of the pressure in the lithosphere from the total lithostatic pressure beneath the ridge (Turcotte and Schubert, 1982). Using both gravitational sliding and thermal models, estimates of the magnitudes of ridge forces per unit length of ridge are found to range from 1×10^{14} to 5×10^{12} N/m, depending on the formulation used to obtain the estimate and values chosen for various thermal constants (Lister, 1975; Richardson, 1976a; Turcotte and Schubert, 1982). As first approximation to this total ridge force acting on the North American plate, a "line-ridge" formulation was used to obtain an idea of the significance of ridge forces in the total driving mechanism.

Line Ridge Forces

Preliminary ridge models were conducted using a line-ridge approximation. In these models, a force per unit length of ridge (subsequently referred to as F_r/ℓ) of 1×10^{12} N/m is applied at the ridge boundary in the direction of relative plate motion. The North American plate is moving clockwise with respect to the Eurasian plate about a rotation pole at 65° N., 132.4° E. at a rate of 0.23° /m.y. (Minster and Jordan, 1978). The total force applied at any node point along the ridge crest is the product of 1×10^{12} and half of the distance between the two adjacent nodes on the ridge. A force of this magnitude applied

over a 5.0×10^3 -m-thick plate produces a stress across the plate of 20 MPa.

The node point locations are converted from constant radius polar coordinates to Cartesian coordinates by the relations:

$$x = \cos(\text{lat}) \cos(\text{long})$$

$$y = \cos(\text{lat}) \sin(\text{long})$$

$$z = \sin(\text{lat})$$

where lat is the latitude and long is the longitude of a given node point. The arc cosine of the dot product of the position vectors in Cartesian space for two adjacent nodes to a node in which a force is being applied are then calculated in order to determine the angular distance between the nodes. The half-arc distance for the two nodes is the appropriate length of ridge corresponding in the intermediate node by which the constant line-ridge force, F_1/ℓ , is multiplied to obtain a total force to be applied at that node.

The force applied at any node is in the direction of relative plate motion between the North American plate and the adjacent plate to the ridge. The relative motion poles are taken from Minster and Jordan (1976). To determine the direction in which to apply ridge forces at each node point, the relative motion pole corresponding to a given node is translated into Cartesian space. The relative velocity for each node point is then calculated as the cross product of the Cartesian position vector for the node and the relative motion pole.

The relative velocity vectors are then translated back into constant radius polar coordinates by the conversion:

$$U_{\text{lat}} = V_x \cos(\text{long}) \sin(\text{lat}) - V_y \sin(\text{long}) \sin(\text{lat}) \\ + V_z \cos(\text{lat})$$

and

$$U_{\text{lon}} = V_y \cos(\text{long}) - V_x \sin(\text{long})$$

The velocity vector, $U_{\text{lat}}, U_{\text{long}}$, corresponding to each node is then normalized and multiplied by the arc distance corresponding to the node. This product yields a vector with a magnitude given by the length (in radians) of the ridge corresponding to a node point that acts in a direction parallel to the relative motion of the two adjacent plates. This vector has a magnitude of 1.0×10^{12} N/m, which is equal to an average stress of 20 MPa averaged across the 5×10^4 -m-thick plate.

As a first approximation to modeling ridge forces, the line-ridge method is sufficient. These forces are shown in Figure 5. Along the elevated region of oceanic lithosphere, however, the total cumulative force should increase from zero at the ridge to a value in the deep ocean basin of similar magnitude to the forces used in the line ridge model. Another shortcoming of the line-ridge model is that the total ridge force corresponding to a certain age of spreading lithosphere is applied on the plate at the spreading center and not at the distance away from the ridge corresponding to this age. Also, ocean bathymetry or ridge topography is not a factor in the line ridge model even though they are essential parameters in a gravitational sliding formulation for ridge forces.

Because ridge forces are related to the cooling and sinking of the plate as it moves from the ridge, the force is not constant

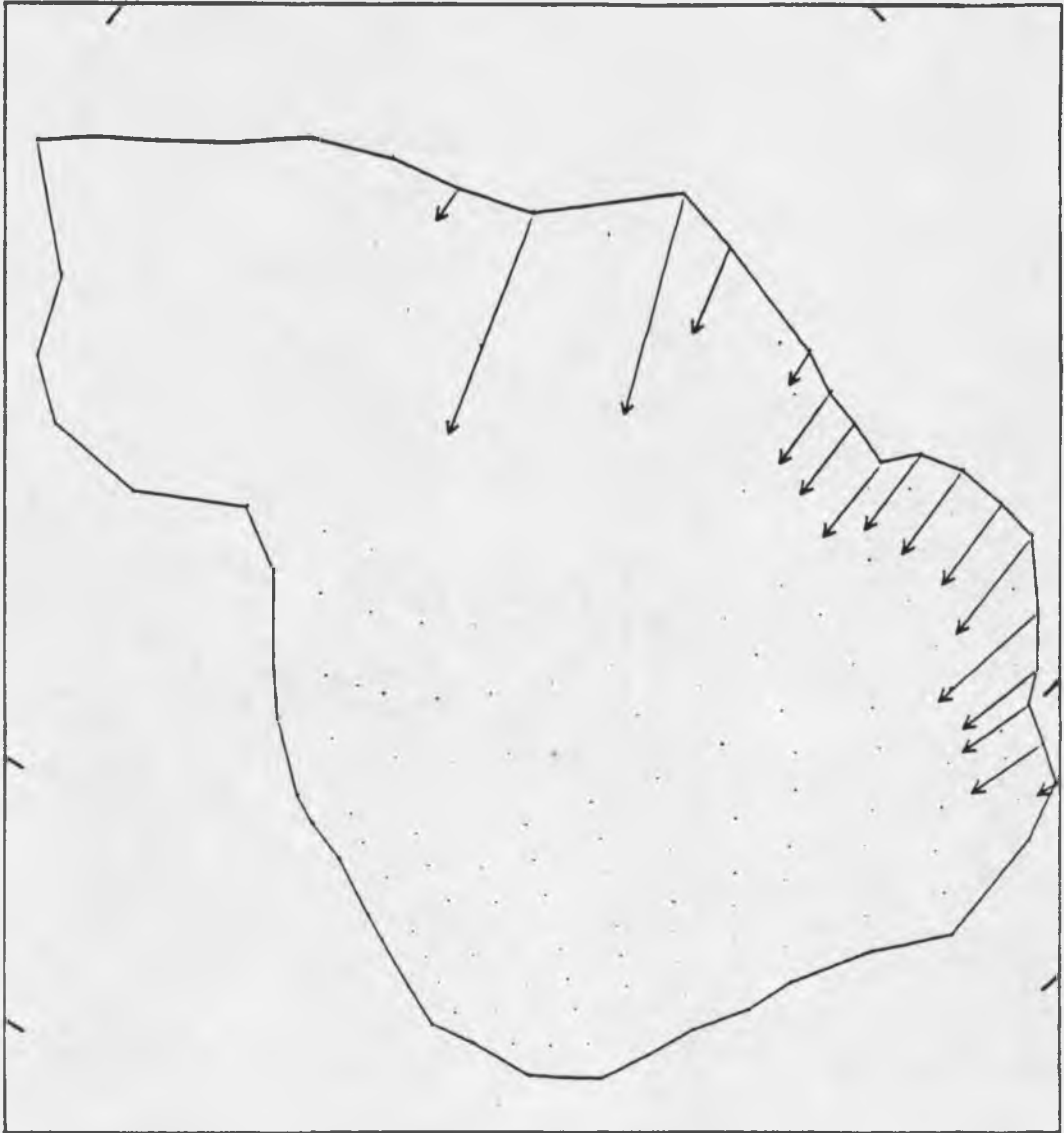


Figure 5. Line ridge forces

throughout the length of the ridge, as assumed by the line ridge model but a function of the distance from the ridge, and so a model that distributes ridge forces through the entire topographic expression of the elevated oceanic lithosphere is a more realistic representation of the potential plate-driving phenomenon.

Distributed Ridge Forces

Distributed ridge force models are designed to provide a more realistic method of modeling ridge forces. Incremental forces are computed for each element of the oceanic lithosphere. The total cumulative ridge force grows with distance away from the ridge. Both a gravitational sliding and a cooling half-space formulation were used to model the distributed ridge forces. Both methods were then compared and contrasted in a test case. Description and procedure of the modeling techniques and the test case follow.

Gravitational Sliding Formulation. Modeling ridge forces as a gravitational sliding phenomenon requires knowledge of lateral density differences due to the cooling, spreading plate sinking deeper into the mantle. The density contrast associated with a certain column of ocean and lithosphere is a function of the cooling history of the lithosphere, which, in turn, depends on the distance of a column from the ridge and the amount of subsidence that has occurred for the lithosphere. This water depth (w) in meters from the ridge level to any point along the lithosphere is found by the relation (Turcotte and Schubert, 1982):

$$w = 5.80 \times 10^{-5} t^{\frac{1}{2}}$$

where: t = age of oceanic lithosphere in seconds
 $= X/v$
 X = distance of spreading center, in meters
 v = spreading rate at ridge .

and reasonable values have been adopted for thermal properties of the plate. A gravitational sliding model is proposed that depends only on water depth as an unknown parameter.

The gravitational force acting on an element in the vertical direction is designated $\Delta F_{\underline{g}} \sin\theta$. The component of $\Delta F_{\underline{g}}$ parallel to the slope of an element is $\Delta F_{\underline{g}} \sin\theta$ where θ is the dip angle from horizontal. Thus, the magnitude of an increment of ridge force depends on the magnitude of θ for a given element. The total ridge force acting on an element of oceanic lithosphere is given by:

$$\Delta F_{\underline{g}} = \Delta\rho gh \sin\theta \text{ area}$$

where: $\Delta\rho$ = density contrast between water and lithosphere,
 \underline{g} = gravitational acceleration
 h = lithospheric thickness
 area = area of an element.

This equation is in agreement with a simplification of Frank's (1972) and Lister's (1975) formulations of the gravitational force. The incremental force per unit length of ridge is:

$$\Delta F_{\underline{g}} = \Delta\rho gh \sin\theta \ell_1 \quad (5-1)$$

where ℓ_1 is the length of the side of an element that is in the local downdip direction, essentially perpendicular to the ridge.

Bathymetric information for each node point in the oceanic lithosphere is used in the finite-element program to obtain the slope of each element, angle θ . The bathymetric data were obtained from a Rand/S10 Global topographic list, which includes averaged bathymetric values for every one degree square on the Earth's surface. Bathymetric values for each node point are interpolated from the encompassing 1-degree rectangles. Each elemental force is distributed equally among the element's three node points. $\Delta F_{\underline{g}}$ is set equal to zero for elements with no net slope. Also, no force is applied to pinned nodes. These forces are shown in Figure 6.

Cooling Half-space Formulation

The ridge forces due to density contrasts are ultimately the results of thermal cooling of the plate. Hence, this force can be described in terms of thermal parameters. The total F_c/ℓ as a function of age from the ridge given by Parsons and Richter (1980) is:

$$F_c/\ell = \underline{g} a \rho_m T_m k t$$

where: a = volume expansion coefficient

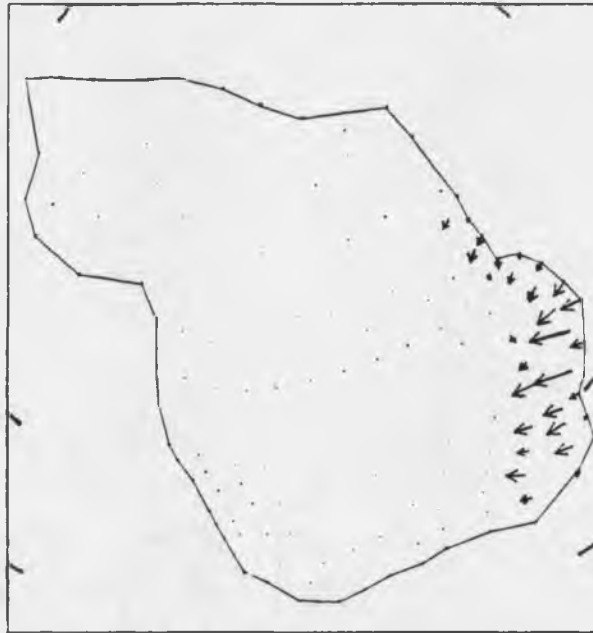
ρ_m = mantle density

k = thermal diffusivity

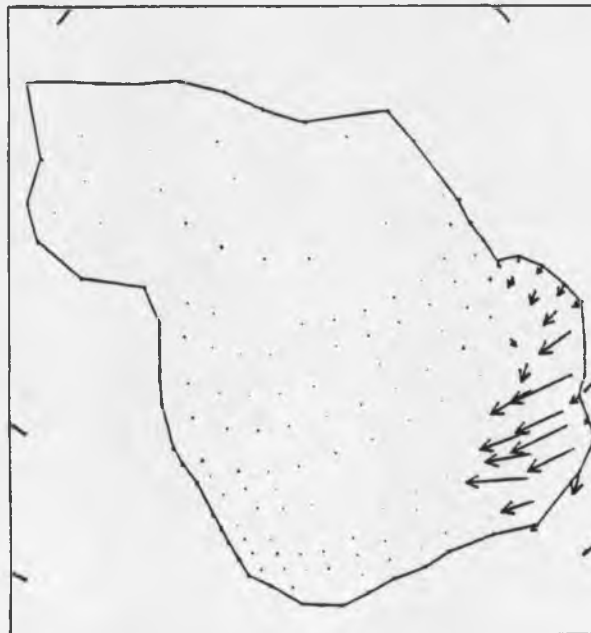
T_m = temperature of mantle.

t = age of the lithosphere.

For $t = 50$ m.y. and reasonable values for k and T_m , the magnitude of



a. Gravitational sliding formulation



b. Cooling half-space formulation

Figure 6. Distributed ridge forces

F_c/ℓ is 2×10^{12} N/m. Thermal models from Lister (1972) and Turcotte and Schubert (1942) yield comparable results.

As in the gravity model, the cooling lithosphere model can be formulated in terms of the known parameter, water depth. Using the relationship for w in terms of t from Turcotte and Schubert (1982):

$$w = \frac{2\rho_m \alpha(T_m - T_o)}{\rho_m - \rho_w} \left(\frac{kt}{\pi}\right)^{\frac{1}{2}}$$

to express the cooling lithosphere formulation, also from Turcotte and Schubert (1982),

$$F_c/\ell = \underline{g}(\rho_m - \rho_w) (w^2/2) + \underline{g}\rho_m \alpha(T_m - T_o) kt$$

in terms of w , an equation for the total F_c/ℓ with no dependence on t results and is given by:

$$F_c/\ell = \underline{g}w^2 \frac{(\rho_m - \rho_w)}{2} \left[1 + \frac{(\rho_m - \rho_w)\pi}{2\rho_m \alpha(T_m - T_o)}\right]$$

Using reasonable values to evaluate the above expression, $F_c/\ell = 3.45 \times 10^1 w^2$ N/m, with w being water depth below ridge crest in meters.

An expression used to calculate incremental forces, $\Delta F_c/\ell$, for each element is obtained as follows:

$$\Delta F_c/\ell \cong F_c(w_1) - F_c(w_2)$$

where: $F_c(w_1)$ = total ridge force per unit length corresponding to the deepest node point of an element at water depth

w_1

$F_c(w_2)$ = total ridge force per unit length corresponding to the shallowest node point of an element at water depth w_2 .

Therefore,

$$\Delta F_c / \ell = 3.54 \times 10^1 (w_1^2 - w_2^2) \text{ N/m}$$

Next, letting $w_1 = \bar{w}$ and $w_2 = \bar{w} - \Delta w$, $(w_1^2 - w_2^2) = 2\bar{w}\Delta w - \Delta w^2$.

Therefore as a first approximation:

$$\Delta F_c / \ell = 7.08 \times 10^1 \bar{w}\Delta w \text{ N/m}$$

where \bar{w} is the average water depth for an element below the ridge where the ridge is assigned a constant depth of 2.5×10^3 m. The total force for each element is calculated by multiplying $\Delta F_c / \ell$ by some fraction of $(\text{area})^{1/2}$ to obtain a force in newtons. The value for this multiplication factor depends on the aspect ratio of any given element. Therefore, by using $\Delta F_c / \ell \times (\text{area})^{1/2}$ as an expression for the total elemental cooling force, $\Delta F_c / \ell$, forces for elements with relatively long sides normal to the ridge will be underestimated and vice versa. These forces are shown in Figure 6.

Ridge Force Test Case. A test case was conducted to compare and contrast modeling results obtained from the line-ridge gravitational sliding and cooling lithosphere formulations previously discussed. A further goal was to choose which formulation would be the best one to use in modeling ridge forces. A test grid (grid 1) was developed, which is highly refined near the ridge and becomes increasingly less

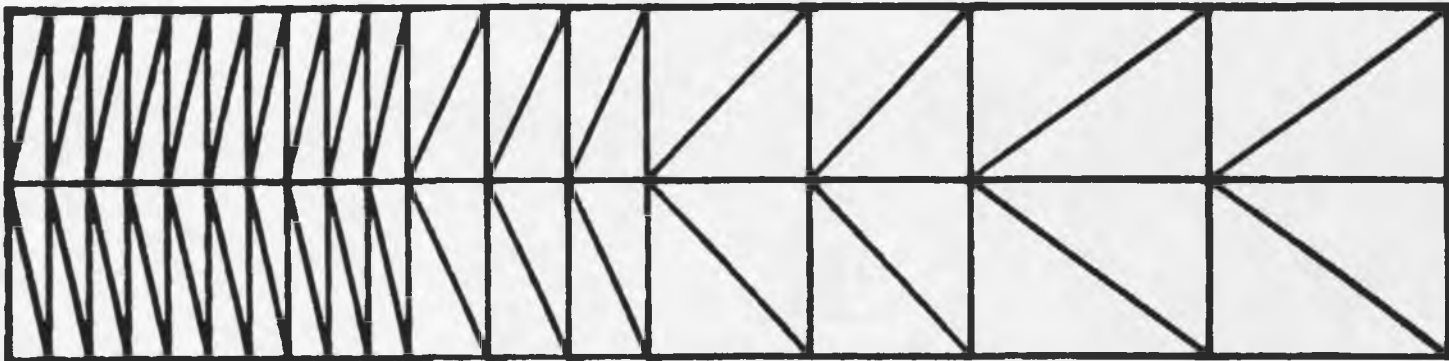
refined away from the ridge. The grid is shown in Figure 7. Nodes on the right boundary of the grid are pinned from motion as well as the top and bottom row of nodes being pinned from motion in the latitudinal directions.

The total length of the grid is 18 degrees, corresponding to a lithospheric age of 80 m.y. for a spreading rate of 2.5 cm/yr. The grid was extended to 80 m.y. because beyond this age the square root law of ridge topography due to thermal contraction of a uniformly flowing material is no longer valid (Lister, 1975). Hence, the cooling lithosphere model is not an accurate approximation for the oceanic lithosphere beyond this point. Beyond this age, the ridge force no longer increases linearly with distance from the ridge but begins to asymptotically approach a maximum value in a similar fashion to the ridge force defined by gravitational sliding.

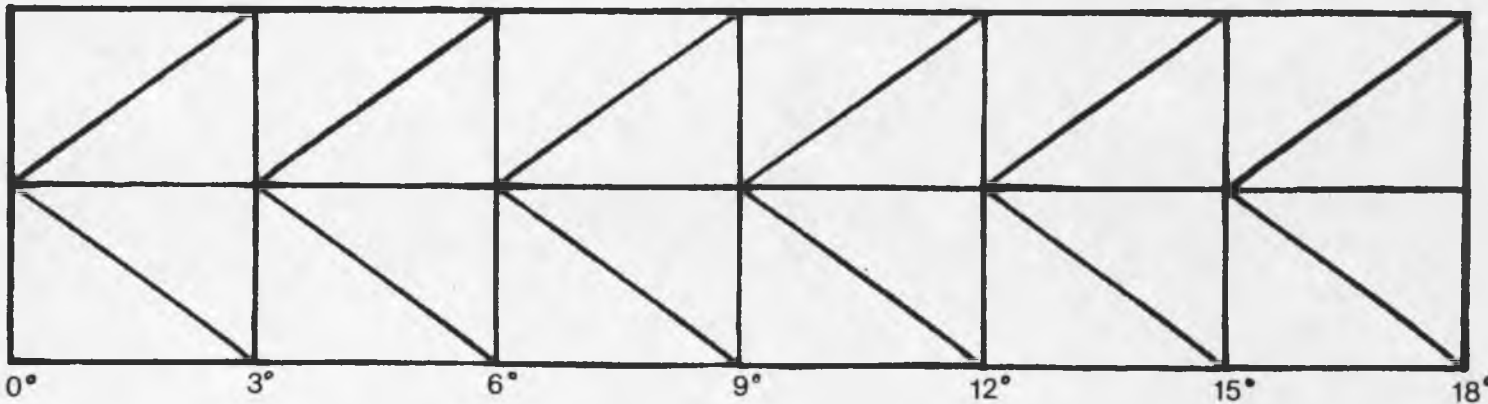
In formulating the test case, it was desired that all models yield equivalent total forces for a 80-m.y.-old oceanic lithosphere. When a lithospheric thickness of 5×10^4 m was used for the gravity model, the total ridge force per unit length, F_r/ℓ , at 80 m.y. for both the gravity and cooling models was 3×10^{12} N/m. The line-ridge forces, being a constant with distance from the ridge, was set equal to this value.

Finally, total F_r/ℓ values at every 10-degree increment away from the ridge were analytically calculated using the following equations:

RIDGE



a. Test grid 1



DISTANCE FROM RIDGE (degrees)

b. Test grid 2

Figure 7. Test grids

$F_{\ell}/\ell = 3 \times 10^{12}$ N/m, for the line ridge model.

$F_c/\ell = 3.54 \times 10^1 w^2$ N/m for the cooling lithosphere model

$F_g/\ell = \Delta\rho gh\bar{w}$ for the gravitational sliding model.

These solutions are plotted in Figure 8.

The gravity equation used to calculate the analytical solution was obtained from the previously derived equation (5-1) for the incremental force per unit length by substituting \bar{w} for $\ell_1 \sin\theta$. Because $\sin\theta = w/X$, where w and X are the total water depth and distance from the ridge for a certain age, $\ell_1 \sin\theta = \ell_1 (w/X)$, which is approximately equal to \bar{w} for small θ .

In Figure 8, the linear dependence of the cooling force on the age of the lithosphere is shown. The change in F_c with X or t is a constant. The gravitational sliding plot indicates that F_g is proportional to X . These results also indicate that $X^{1/2}$ dependence of water depth with distance from the ridge that suggests a parabolic shape for the ocean-lithosphere interface.

Stress is equal to force/area. However, to determine the resulting stresses from the nonconstant analytic gravitational and cooling force solutions in the test case, the change in F_r/ℓ with distance for both models had to be integrated over the nodal distance.

The stresses were calculated using the expression:

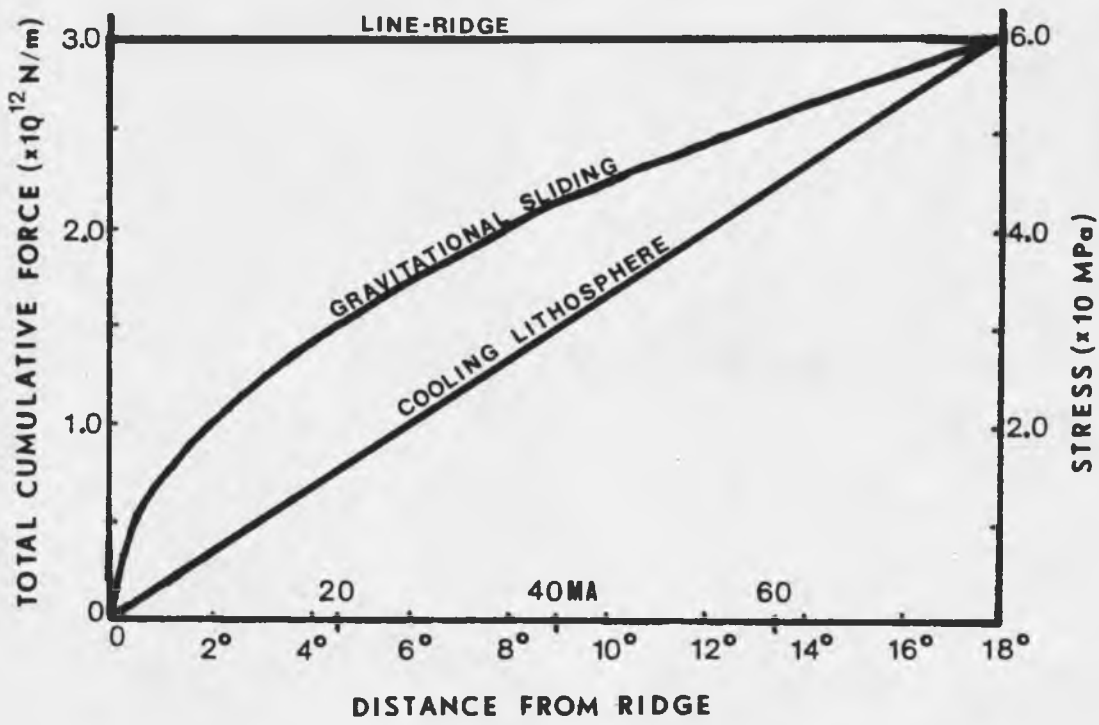


Figure 8. Total cumulative forces and stresses from ridge force test case

$$\sigma(x) = \frac{1}{h} \int_0^x ((\partial F_r / \partial x) \partial x) \partial x$$

The stresses for all three force models were found to increase with distance away from the ridge in the same fashion as the forces (Figure 8).

The same test was conducted using the computer algorithms previously discussed. The results for both the cooling and gravity models show that the computer-calculated forces when summed together, accurately match the analytical solution with only one stipulation. Incremental forces for an element are calculated as functions of area and the total change in water depth across the element. Although the calculated elemental forces may best be assigned to the element centroid, the best agreement of the analytic with the calculated solutions is obtained when the forces are plotted at the age or distance corresponding to the deepest node point. The computer-calculated elemental stresses for all three models for an element are then plotted at the distance corresponding to the element centroid (Figure 8). These stress values reasonably approximate the analytically determined stresses.

In conducting this test case, the actual values for ℓ were included instead of using the approximation for ℓ_1 of $(\text{area})^{\frac{1}{2}}$. A second test grid (Figure 7) with elements of comparable dimensions to the coarse grid (Figure 4) ridge element was used to test whether these elements could sufficiently approximate the curvature of the lithosphere near the ridge. The approximation of ℓ_1 in terms of area and the large element sizes near the ridge were found to be sufficient to yield force

and stress results for all three force models approximately equal to both the analytical and computer solutions from the first test case.

Continental Topography Forces

In addition to ridge forces, forces acting on the lithosphere, arise from density heterogeneities in the continental crust and upper mantle. As to the case for the elevated ridge, potential energy is stored in elevated continental regions as well as in compensating root systems. This gravitational potential associated with crustal thickness variations yields a horizontal force that acts to reduce the thickness heterogeneities in the continental crust. According to Artyushkov (1978), the stresses related to varying crustal thicknesses, and consequently lateral density inhomogeneities, range from a few tens to a hundred MPa. In addition, the compressive stresses induced by the cold root of a mountain are alone able to sustain mountain-building processes independent of transmitted forces from a great distance, i.e., from the ridge. Stress orientations in the northern Appalachian and Rocky Mountains are inconsistent with the broad east-northeast compressive stress trends of the stable continental interior (Zoback and Zoback, 1980) and indicate that in addition to the ridge force a force or forces related to mountain systems is possibly acting on the continental lithosphere.

Analysis of intracontinental stress states due to topography requires consideration of lateral variations in the mechanical properties, density contrasts, and geometrical constraints for the lithosphere (Fleitout and Froidevaux, 1982). A formulation dependent on unknown

parameters similar to those in the gravitational sliding ridge force formulation was sought that would express horizontal stress in the continent as a function of continental topography and lateral density differences.

The horizontal force per unit length due to lateral differences in density is the integral evaluated from the topographic values to the compensation depth, d , of the difference between the lithostatic pressures for a lithospheric column and a reference column. This force expression is given by (Richardson, 1978b):

$$F = \int_{\text{topo}}^d P_R(z) - P_L(z) dz \quad (5-2)$$

where P_R = pressure in the reference column

P_L = pressure in an arbitrary lithospheric column.

This pressure, $P(z)$, related to the weight of overlying material at a given depth z can be expressed as:

$$P(z) = \int_{\text{topo}}^z \underline{g}\rho(z') dz' \quad (5-3)$$

where $\rho(z)$ is the density at depth z . Similarly, the average vertical stress in a column of lithosphere is related to the difference in the lithostatic pressure in the column and a reference column and is expressed as:

$$\sigma_{zz} = \frac{1}{d} \int_{\text{topo}}^d \underline{g}\Delta\rho(z) z dz$$

where $\rho(z)$ is taken to be $(\rho_{\text{reference}} - \rho_{\text{column}})$ in order to comply with the convention used in the gravity sliding modeling for a ridge in which a force impressed on an oceanic column from a ridge reference column has a positive sign. If σ_{zz} is positive in a given column, the column is exerting a radially outward force, which acts to compress surrounding lithosphere and create a state of deviatoric tension with respect to the reference column in the column itself.

A physical quantity known as density moment has a value that is a function of crustal thickness and topography. Crustal thickness and topography are ideal model parameters with which to formulate an expression for horizontal stresses due to crustal thickness inhomogeneities for the continental and shelf portions of the plate. An expression for σ_{zz} in terms of these two parameters thus yields an expression of σ_{zz} in terms of moment M . Fleitout and Froidevaux (1982) related σ_{zz} and M by the equations:

$$M = \int_{\text{topo}}^L \Delta\rho(z)zdz \quad (5-4)$$

The physical significance of the density moment is apparent by comparing equations (5-2) and (5-4). The quantity (Mg) is thus a horizontal force per unit length equivalent to the force expression in terms of pressure differences (equation 5-2).

To model these forces related to the density moment for continental lithosphere, crustal thickness values for each node point are interpolated from a global thickness map (Soller, Roy, and Brown, 1983). This map is a contoured compilation of various crustal thickness

determinations from surface wave refraction studies. Contoured crustal thicknesses are shown for the North American plate in Figure 9. In addition, topographic values for the same nodes were obtained from the same global data set and were interpolated in the same fashion as the bathymetric data for the oceanic lithosphere. A three-dimensional plot of topographic and bathymetric values for the plate was generated to visualize the relative differences in elevation throughout the plate that contribute to some form of gravitational sliding forces. The plot (Figure 10) is on a Mercator projection, and therefore areas near the north geographic pole (top of figure) are highly distorted.

In the modeling scheme developed to evaluate these forces, the density moments for each element were calculated using equation (5-4). The average topographic and crustal thickness values for each element were first evaluated from the three nodal point parameters. Each element can be thought of as a vertical column having a certain elevation above or below sea level, a certain crustal thickness, which includes topography and a resultant mantle thickness equal to the compensation depth minus the crustal thickness below sea level. A reference column or element representing the vertical density structure of the Mid-Atlantic Ridge was used in the modeling scheme. The reference column includes 2.5×10^3 m of water of density 1.03×10^3 km/m³, no crustal material, and a constant mantle density of 3.23×10^3 kg/m³ for a total thickness of 1×10^5 m for the column. The mantle density value was chosen so that the reference column would have the same weight as the ridge reference columns of Hess (1972) and Fleitout and Froidevaux (1983).

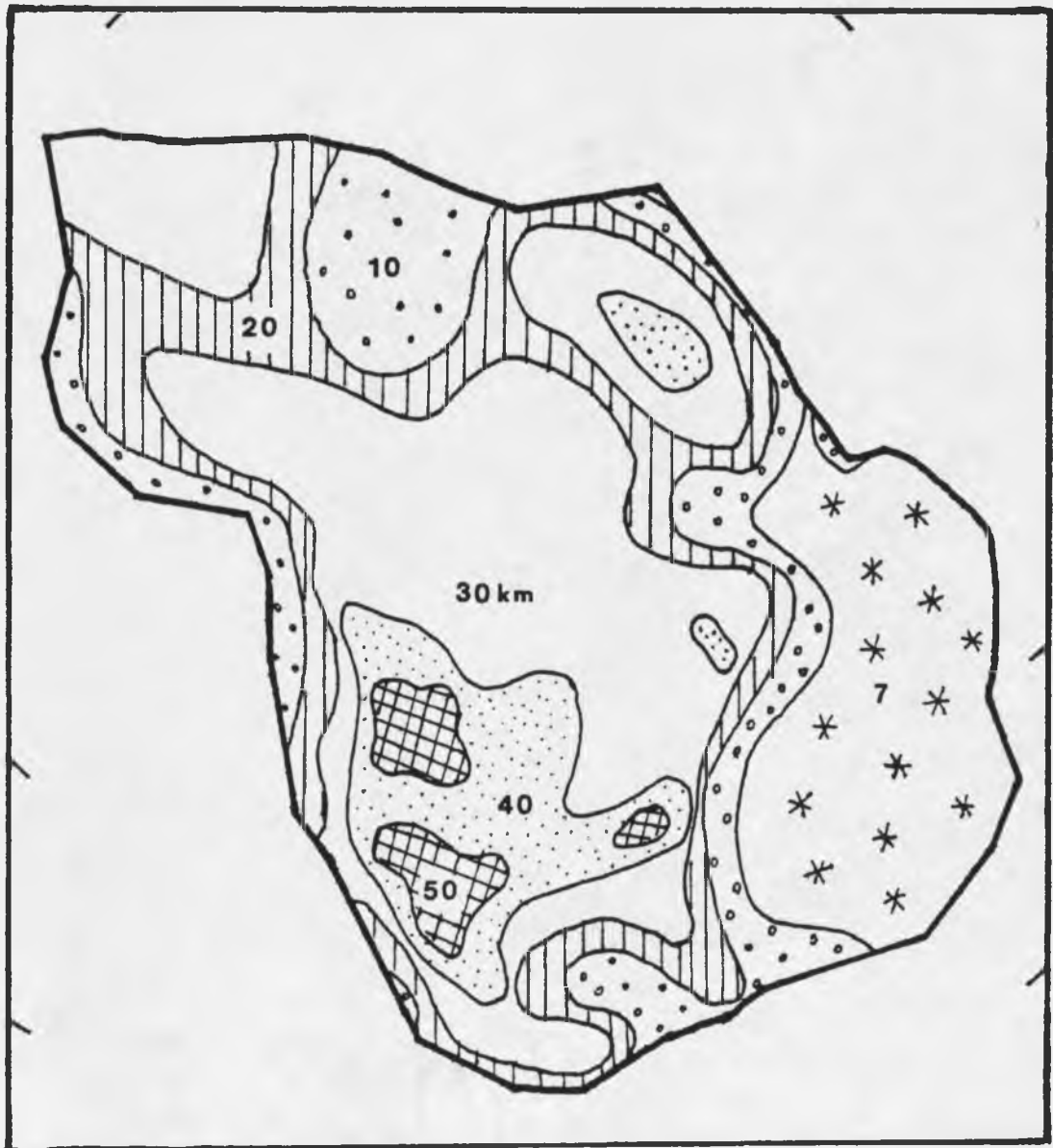


Figure 9. Contoured crustal thicknesses for North American plate. -- From Soller and others (1982).

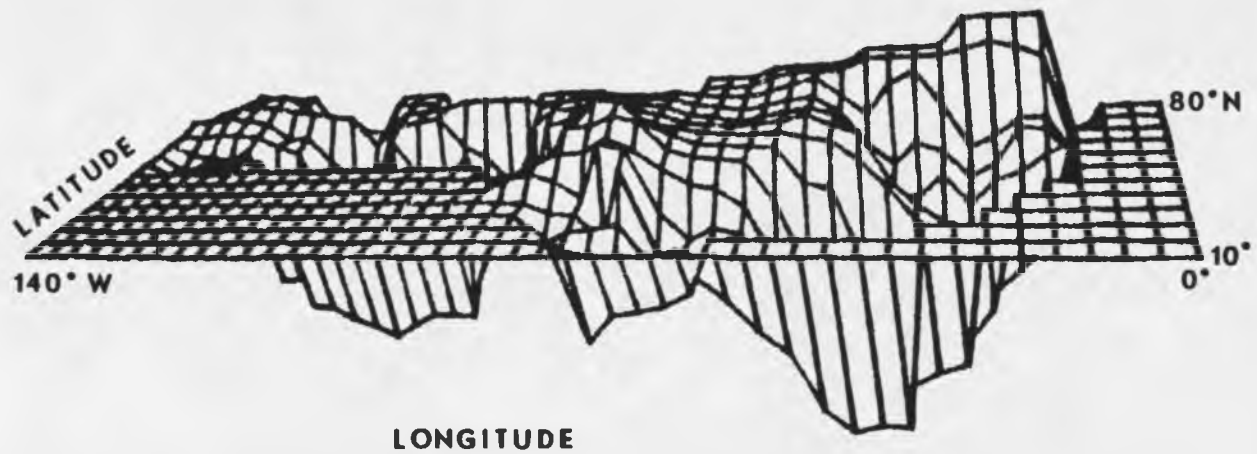


Figure 10. Three-dimensional topography of the North American plate on a Mercator projection

By assuming an oversimplified crustal density structure--a constant density of $2.76 \times 10^5 \text{ kg/m}^3$ for all continental crust--an average mantle density for each elemental column can be calculated by equating the average density for the whole column with that of the reference. Thus, in this approximate model of the vertical density structure for the continental portion of the plate, a constant density for all crust was assumed and a variable mantle density was established that enables all elemental columns to be in isostatic equilibrium with the reference column and hence with each other.

Once a horizontal force per unit length equal to (Mg) is calculated for an element, it is applied in the direction normal to the three elemental faces. The force per unit length acting in the directions of the three unit vectors normal to the faces is converted to a total force by multiplying the three radial forces by the length of their corresponding side. The normal unit vectors and the vectors between node points for each element are determined in a local X,Y plane by ignoring any component in the Z direction, because the horizontal force for an element corresponds to a constant average elevation and crustal thickness in the Z direction. The sum of the three radial forces for an element in its local coordinate system should equal zero in order for the column to be in equilibrium. These force components are then transformed into the global coordinate system for the plate. It is the addition and subtraction of radial forces from adjacent elements that produces net forces that act in gradient directions to minimize potential energy associated with crustal thickness inhomogeneities of the continental lithosphere.

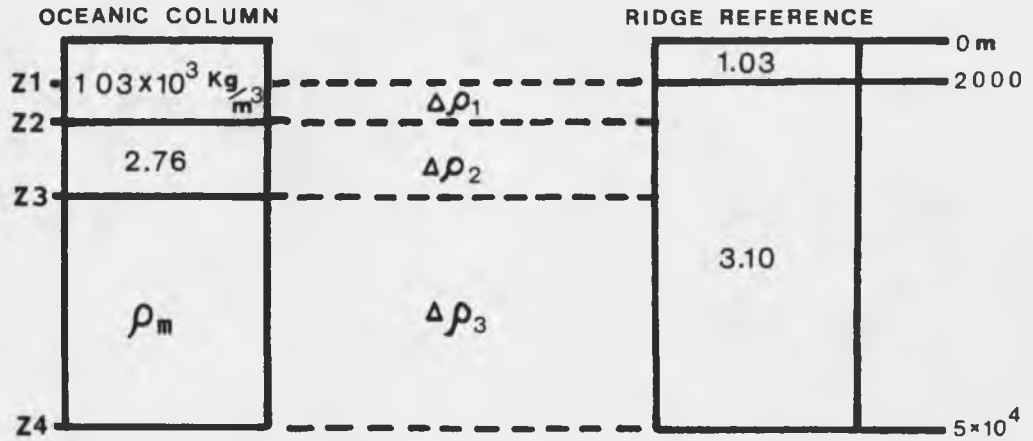
Continental Topography Force Test Case

Before modeling continental forces due to density heterogeneities was done, a test case was conducted that used the density moment formulation to approximate ridge forces. As in the gravitational sliding and cooling half-space formulations, the moment equation depends on bathymetry. Also a constant thickness of 5×10^4 m was used for the oceanic lithosphere; the compensation depth was also at 5×10^4 m. The ridge reference column included 2.5×10^3 m of ocean with the rest of the column down to 5×10^4 m being a constant density, 3.1×10^3 kg/m³, mantle material. This average mantle density for a 5×10^4 -m-thick column was also ascertained from various cited density models of a ridge (e.g., Hess, 1972; Fleitout and Froidevaux, 1983). However, the moment equation is an integral of vertical density contrasts between an oceanic column and the ridge reference, unlike that gravitational sliding formulation, which assumes a constant density for all oceanic lithosphere and uses only the contrast between this density and that of the ocean to determine the gravitationally induced force due to change in water depth from the ridge to any oceanic lithosphere element. Substantial differences in these two approximations for ridge forces exist, but it is difficult to determine which approximation allows for a more accurate and realistic method of modeling ridge forces.

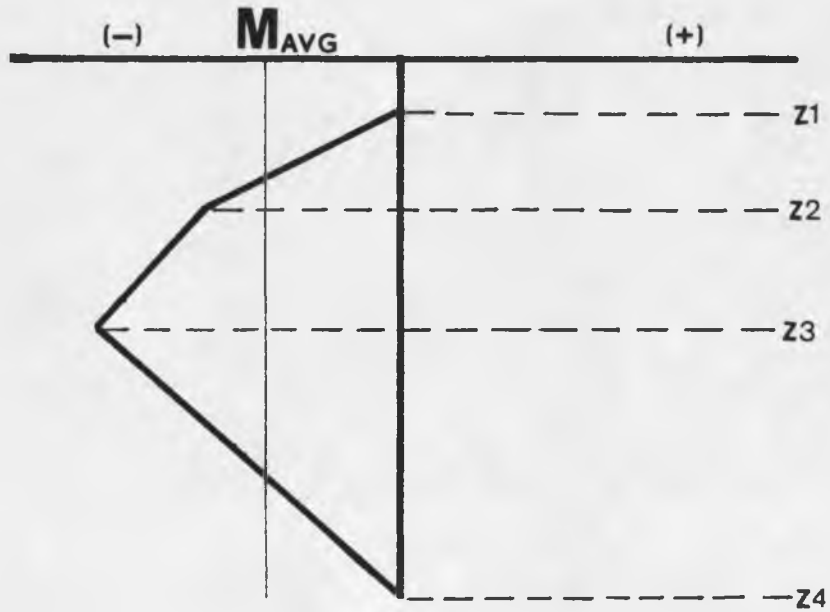
A total cumulative force at 80 m.y. was determined from calculated density moments for the test grid elements of Figure 7 to compare the magnitude of this total force with the presently determined 3×10^{12} N/m total force value for that age (see ridge force test case). In this test case, horizontal density contrasts and hence horizontal forces for

the oceanic lithosphere were found to be highly dependent on the density profile used for the elemental columns. The density moment scheme, which produced total cumulative forces away from the ridge of approximately 9×10^{12} N/m, had a constant oceanic crustal thickness of 7 km with a 2.76×10^3 kg/m³ density. The mantle material was determined to satisfy isostasy. This total force magnitude is three times larger than that predicted by a cooling half-space; therefore, the assumptions made about the density structure of the oceanic lithosphere were not accurate.

All of the calculated moments for oceanic lithosphere had a negative sign. This sign was dependent on the convention chosen to calculate $\Delta\rho$, i.e., $\rho_{\text{ref}} - \rho_{\text{col}}$. The sign convention is related to the moment vector about some origin point but is arbitrarily chosen to satisfy the direction of forces acting on oceanic lithosphere from the ridge. All columns with associated negative moments are modeled to have radially inward forces acting on the column that compresses the column. Positive moments yield radially outward forces, which produce tension in a column. Figure 11 is an illustration of an arbitrary oceanic column and the ridge reference column. Also shown is a plot of the density moment for the oceanic column as a function of depth z . As the graph illustrates, the ridge is applying a radially outward force proportional to the moment, M , which acts to compress the oceanic column through the entire thickness of the column. This force increases until it reaches a depth where M is maximum; then the ridge force decreases until there is no force at the base of the oceanic column from



DENSITY MOMENT (kg/m)



$$M_{AVG} = \int_{Z1}^{Z2} \Delta\rho_1 y dy + \int_{Z2}^{Z3} \Delta\rho_2 y dy + \int_{Z3}^{Z4} \Delta\rho_3 y dy$$

WHERE $\Delta\rho_i = \rho_{ridge} - \rho_{ocean}$

Figure 11. Schematic of the density moment for an oceanic column

the ridge and both columns are in isostatic equilibrium. M_{avg} is the value of the density moment for the oceanic column with respect to the ridge column. A number of test cases were developed to test the roles of crustal thickness and topography on density moments. In one test case, continental lithosphere was assigned a constant crustal density of $2.76 \times 10^3 \text{ kg/m}^3$. The continental mantle material was also assigned a constant density that satisfied isostasy. The continental lithosphere was chosen to be $1 \times 10^5 \text{ m}$ thick. The ridge reference column was extended to $1 \times 10^5 \text{ m}$ also. The test was conducted to simulate the situation of a point or element mass having a positive elevation with respect to surrounding reference elements; the horizontal force and resulting stresses induced by the elevated topography were analyzed. The elevated region was found to be in a state of deviatoric tension, because the density moment for this column was positive, which resulted in radially outward horizontal forces for the element. Consequently, surrounding elements were in a slight state of compression, and elements farther from the elevated ones became more compressional in order to balance the loads impressed on the surrounding elements due to the potential that the elevated topography had to spread out. This test also revealed that the addition and cancellation of radial horizontal force components resulted in net force directions along density inhomogeneity gradients. So, unlike oceanic lithosphere, which appears to be in a state of compression due to the ridge, continental highs appear to have a potential to spread out.

The results from these density moment test cases revealed the general, oversimplified effects of positive and negative relief with

respect to the ridge on density moments and resulting horizontal forces. In both tests, the effect of varying crustal thicknesses was ignored but was investigated in a third test case. This test was designed such that adjacent elements increased in thickness from 5×10^4 m to 1×10^5 m in 1×10^4 m increments. Topography was held constant at sea level for each element. The result from this test revealed that the thinner crustal columns induced an increasingly greater force on the thicker columns so that the stress states in the test grid varied from extensional tectonics in the thinner crustal columns to compressional features in the thicker columns. In fact, the influence of varying crustal thickness on the moment magnitudes in general appears to outweigh the effects of topographic variations for the North American plate. It can be observed on Figure 12 that the stresses in regions in which crustal thickness values are constant are a function of density variations due to topography changes; however, in areas where crustal thicknesses are changing, horizontal forces tend to be oriented along gradients of the thickness contrasts and in the direction of the areas with greatest crustal thickness. Thus, even though topographic highs appear to have a tendency to expand, as was illustrated in the second test case, the large crustal thicknesses usually associated with high topographic relief result in compressional instead of tensional stress states for high regions of the continent. This effect possibly explains why not all mountainous or elevated regions on the continent are characterized by extensional tectonics.

Elemental columns for the continental lithosphere were modified such that mantle densities at the base of the lithosphere were equal to

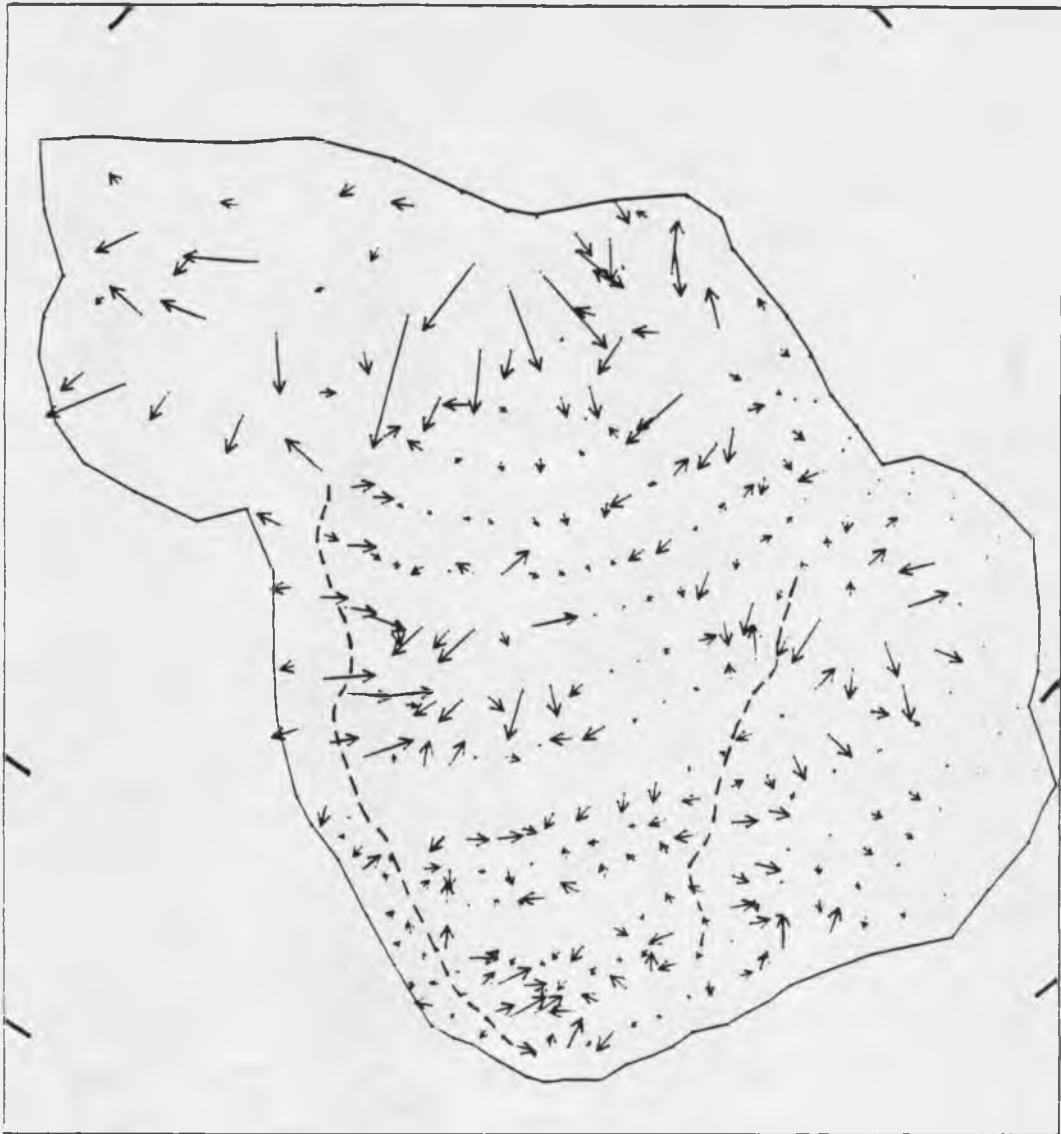


Figure 12. Geoid undulations referred to the hydrostatic flattening of $1/299.638$. -- After Nakiboglu (1982). Potential coefficients complete to degree 180. Contour interval of 5 m based on $2^\circ \times 2^\circ$ grid.

the relatively low mantle density of the ridge reference column, or 3.23×10^3 kg/m³. As was discovered when conducting the test cases, the deeper mass anomalies are concentrated in a lithospheric column, the larger the associated density moment. Decreasing the mantle density with depth, however, raises the center of the mass anomaly, and because density moment is a function of depth squared, this decrease reduces the resultant stress magnitudes by at least half an order of magnitude. It is because of this dramatic effect of density anomalies at depth and the supposition that continental root systems are compensated by very high, shallow upper mantle densities that the mantle layer in continental columns is divided into two layers. As a first approximation to modeling the questionable mantle density structure under continental crust, the lower half of the mantle lithosphere was assigned the constant density of 3.23×10^3 kg/m³ and the density for the upper half was chosen to satisfy isostasy.

Continental Topography Related to the Geoid

It is apparent that in using a density moment scheme to model the effects of continental topography on the tectonic stress regime of the North American plate, bold assumptions and generalizations must be made as to the density structure of the lithosphere. The models are highly dependent on the reference profile, compensation depth, crustal thicknesses, and the nature of the mantle geotherm assumed for the plate. For the continental portion of the plate, reasonable attempts to model the effects of density heterogeneities were tested. The only

constraint to these moment magnitudes for the continental lithosphere can be obtained from information about the geoid.

Geoid anomalies have been shown to be a function of dipole moments of density distributions in the crust and upper mantle (Haxby and Turcotte, 1978; Parsons and Richter, 1980; Turcotte and Schubert, 1982). Figure 13 is a contoured map of undulations in the geoid. Numerous factors such as thermal structure of the lithosphere and glacial phenomena contribute to the nature of these contours. Deep long-wavelength features generally control undulations in the geoid. However, short-wavelength shallow features in the lithosphere such as thickness inhomogeneities can cause slight deviations in the trends of the long-wavelength contours. These deflections across continental margins can be used to determine how the geoid changes along traverses normal to continental margins and hence how moment magnitudes along these traverses should differ.

In fig. 13, contours due to long-wavelength features fortuitously traverse the Australian continent normal to its eastern and western continental margins. Deflections on the order of 10 m can be observed. Unfortunately not all deviations of contours can be observed for continental margins of all continents, especially the Atlantic coastal margin of North America. However, 10 ± 5 m is accepted as a good estimate for a change in the geoid anomaly across almost all continental margins (Chase, 1984, personal commun.). The difference in the moment magnitudes between a characteristic continental shelf column and a coastal plain column was computed and compared to the difference in

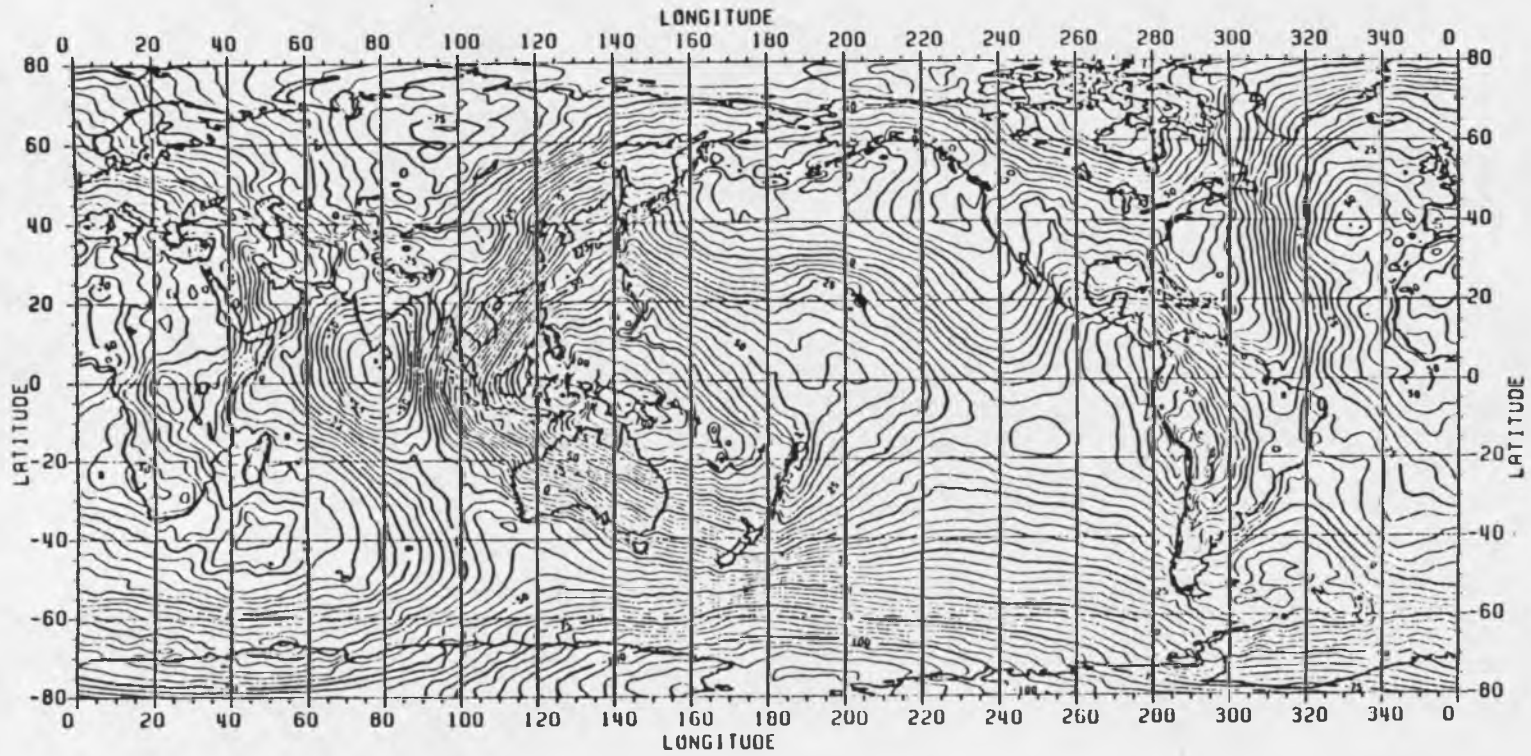


Figure 13. Continental topography forces based on density moments

the density moments expected by an assumed 10-m geoid anomaly between the two columns.

From Parsons and Richter (1980), an expression that approximates the geoid anomaly relative to the ridge crust is given by:

$$N = \frac{2\pi G}{g} \int_0^L \Delta\rho(x, z) dz = \frac{2\pi G}{g} M \quad (5-5)$$

where: G = gravitational constant

$\Delta\rho(x, z)$ = difference in the vertical density profile for a column at a distance x from a ridge reference column.

From equation (5-5) and calculated values for the density moments of a characteristic coastal plain column and a continental shelf column, a value for the geoid anomaly expected between these two columns was determined. An anomaly of 7 ± 2 m was calculated and found to reasonably agree with observed anomalies that occur over the area between the coastal plain and shelf regions of the Atlantic coastal margin of North America (Figure 13).

As a result of this conclusive evidence, the density moment formulation used to model topography forces due to lateral density inhomogeneities in the continental crust is believed to yield density moments of relatively accurate magnitude. These forces are shown in Figure 12.

Transform Boundary Forces

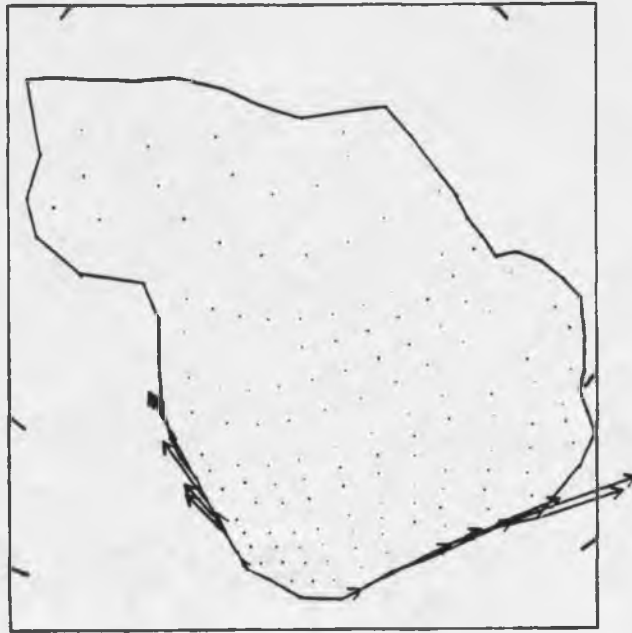
A substantial portion of the North American plate is bounded by transform faults. Along these transform boundaries, the relative motion

between adjacent plates is resisted. The relative motion vectors at most transform boundaries are essentially parallel to the boundary, as they are for the San Andreas transform boundary and the boundary between the Caribbean and North American plates. The magnitudes of shear stresses along the transform boundary segments of the plate are uncertain. These magnitudes are influenced by a combination of rock properties and ambient stress conditions. Transform boundaries, especially the Caribbean transform, possibly provide balancing resistance to the ridge forces.

Transform forces were applied along the Caribbean and San Andreas boundaries, antiparallel to the relative motion vectors of the North American plate with the Caribbean and Pacific plates, respectively. These forces are shown in Figure 14. A constant arbitrary force per unit length was applied at each node point along the transform boundary. Total forces were computed as a force per unit length multiplied by the length of the boundary over which the force acts. The magnitude of the force per unit length depends on assumptions made about the magnitude of shear stresses along the boundary.

Caribbean Transform Boundary

The relative rate and direction of movement of the Caribbean plate with respect to the North American plate can be determined from the slip vectors of shallow earthquakes that occur along the transform boundary. In general, the North American plate is moving in a westerly direction with respect to the Caribbean plate. The Caribbean plate is a small bufferlike plate between the North and South American



a. San Andreas and Caribbean transform forces



b. Aleutian and Cocos convergence forces

Figure 14. Boundary forces for the North American plate

plates, and its motion is essentially controlled by the motion of these two surrounding plates. The tectonic processes occurring along the boundaries of the Caribbean plate are quite complicated and not well understood. Numerous angular velocities and rotation poles have been proposed for the plate. One of the major difficulties in determining these parameters is that, with respect to North America, the Caribbean boundary changes from transform at the Mid-Cayman spreading center south of Cuba to a transitional type of boundary near Puerto Rico and finally to a subduction zone complex along the Lesser Antilles. For simplicity in modeling and because the length of the segment of the subduction boundary is relatively insignificant, forces related to this subduction process are not considered in the modeling.

Motion along the northern side of the Caribbean plate appears to be distributed along more than one major fault system (Sykes, McCann, and Kafka, 1982). Discrepancies in estimated angular velocities and rotation poles are due to the various motions of different segments of the northern boundary. Minster and Jordan (1978) used magnetic profile data across the Mid-Cayman rise to determine a relative motion pole and rotation rate for the Caribbean-North American plate pair. They do not consider slip vectors from the Puerto Rico trench and Hispanola regions where they believed the stress and strain fields are complex and that data show internal scatter. Sykes and others (1982) believed that Minster and Jordan's rate and rotation pole represent only a portion of the relative motion between the two plates. Sykes and others claimed to have obtained a more accurate estimate of the full rate of motion along the northern Caribbean boundary. They

demonstrated that the North American plate is moving in a west-southwest direction along the Puerto Rico trench at a rate of $0.36^\circ/\text{m.y.}$ clockwise about a center of rotation at $66^\circ \text{ N.}, 132^\circ \text{ W.}$ According to Minster and Jordan (1981), the North American plate is moving counterclockwise with respect to the Caribbean plate about a pole at $-33.8^\circ \text{ W.}, -70.5^\circ \text{ E.}$ at a rate of $0.29^\circ/\text{m.y.}$

The relative plate motion information of Minster and Jordan (1981) was used in modeling shear tractions along the Caribbean-North American boundary because a more simplified relative motion model, as used in this modeling scheme, was assumed to arrive at the motion parameters and because the relative plate velocity obtained from using Minster and Jordan's pole are approximately parallel to the transform boundary.

San Andreas Transform Fault

Another major transform boundary of the North American plate is the San Andreas fault, which marks the southern portion of the boundary between the Pacific and North American plates. Along this fault system, the North American plate is moving in a southerly directions with respect to the Pacific plate. With respect to the Pacific plate, the North American plate is moving counterclockwise at a rate of $0.5^\circ/\text{m.y.}$ about a pole of rotation at $48.8^\circ \text{ N.}, -73.9^\circ \text{ E.}$

Some estimates of the magnitudes of the shear stresses along the San Andreas fault have been made. Heat-flow measurements across the fault, along with a model of shear heating, indicate that a maximum shear stress of a few tens of MPa is acting on the fault (Brune,

Heney, and Roy, 1969; Lackenbruch and Sass, 1980). Zoback and others (1980) suggested that the mean shear stress on the fault exceeds several tens of MPa at seismogenic depths.

The Juan de Fuca plate, west of the State of Washington, is a small platelet between the Pacific and North American plates. It is believed to be spreading away from the Pacific plate and subducting beneath the North American plate; however, recent coupling of the plate with the North American plate is also possible (Atwater, 1970). Because of the small size of the Juan de Fuca plate and its questionable tectonic relation to the North American plate, no boundary forces were included along this segment of boundary.

Even though significant relative motion exists between North and South America according to Minster and Jordan (1978), observational evidence, i.e., seismic activity, is minimal. For this reason no forces were applied along the segment of the North American boundary marking the distinction between the two American plates.

Normal Forces

A major shortcoming in single-plate modeling is that tectonic forces acting on a plate from outside the plate's boundaries are not incorporated into a modeling scheme that approximates the tectonic forces due to tectonic mechanisms associated with the plate alone and act within and on the periphery of the plate. Some potentially substantial forces transmitted from neighboring plates, which may be acting on the North American plate, are normal forces at transform boundaries and forces related to the subduction of adjacent plates beneath the

North American plate. Specification of these forces is not straightforward; these transmitted forces depend not only on boundary type but on global stress patterns (Richardson, Solomon, and Sleep, 1976).

For forces normal to transform boundaries, Forsyth and Uyeda (1975) suggested that the sign of these boundary forces cannot be assessed without prior knowledge of the other stresses acting on the plate. They also believed that large normal forces could not exist without causing a substantial readjustment to the relative motion of the plate. However, in modeling the North American plate, the incorporation of some semblance of these transmitted forces from neighboring plates appears to be a necessary boundary condition in order to realistically represent the tectonics of the plate. Forces normal to the San Andreas and Caribbean transforms were applied at each node point perpendicular to the transform force for that node such that the normal force vectors pointed inward on the North American plate. For an initial approximation, the magnitude of the normal force at a node point was set equal to the corresponding transform force.

Convergence Forces at Subduction Zones

A second type of force transmitted from an adjacent plate to the North American plate occurs along subduction zones. Along the Aleutian arc complex and the Cocos boundary, portions of the North American plate are overriding the Pacific and Cocos plates, respectively. Whether the subducting slabs attached to the Pacific and Cocos plates are transmitting compressive stresses to the overriding North American plate or whether the upper plate is being pulled toward the trench,

forces approximately parallel to the relative motion between the subducting plate and the North America plate probably exist. The mechanics of plate collision at a subduction zone would suggest that some sort of suction force on the overriding plate may exist from the trench due to the void of material caused by the subducting slab (Forsyth and Uyeda, 1975). However, because this is a zone of convergence, each plate is essentially pushing on the other so a net compressive force on the overriding plate could result. Or the pull of the North American plate into the trench could simply be due to the ridge force pushing the plate into the trench from the ridge. Basically, regardless of whether the overriding plate is being pulled toward or pushed away from the trench, it is probably the net effect of this unknown convergence force with the ridge force across the plate that produces the observed stress states in the north and southwest corners of the North American plate.

Aleutian Convergence Forces

Despite the localized tensional character of earthquake foci observed beneath the Aleutian trench (Stauder, 1968), which are probably located in the subducting plate, the general tectonic stress states observed farther inland from the trench are compressional with maximum compressive stresses oriented approximately parallel to the relative velocity vectors of the Pacific and North America plates (Nakamura and others, 1977; Jacob and Perez, 1982). Initial models of the forces acting along the Aleutians due to Pacific plate subduction have forces pointing toward the interior of the North American plate parallel to the

relative motion between the plates. The magnitude of these forces is arbitrary but was initially chosen to have the same magnitude per unit length of boundary as the transform forces. The relative motion pole and counterclockwise rate of rotation of the North American plate with respect to the Pacific plate are 48.8° N., -78.9° E. and 0.85° /m.y., respectively (Minister and Jordan, 1978).

Cocos Convergence Forces

The Cocos plate is subducting beneath the North American plate along Mexico in a relative direction approximately N. 58° E. (Chael and Stewart, 1982). Compressional tectonics are also observed inland from the Cocos-North American plate convergence boundary. Therefore, transmitted compressional forces from the Cocos plate were incorporated into the modeling scheme. These forces were applied in a direction away from the Middle American trench in directions parallel to relative motion vectors. The relative rotation pole and rates of the Cocos plate with respect to the North American plate were given by Minister and Jordan (1978) as 29.8° N., -121.3° E. and 1.49° /m.y., respectively. The convergence forces at the Aleutian and Cocos subduction complexes are shown in Figure 14.

Drag Forces

The flow pattern of asthenospheric material is the most crucial phenomenon to understand to be able to accurately assess and understand the driving mechanism for plate tectonics. Unfortunately, this phenomenon is poorly known and the subject of much debate. A contrast in the viscosity of these two layers results in the existence of

viscous shear forces at the base of the plates, if in fact the plates are moving with respect to the asthenosphere. These shear forces may either contribute to the plate-driving mechanism, or they may act to resist such a process. The direction of these forces depends on the relative velocity between the surface plates and sublithospheric mantle flow. The magnitude of the forces depends on plate velocity and area and the viscosity of the asthenosphere.

Driving Drag

Flow of mass in the asthenosphere is essential to balance the mass transport of the North American plate as it moves from the ridge. This mantle counterflow is obviously not simple and uniform as evidenced by the variable rates, sizes, and boundary types of the surface plates. Mantle convection is one possible mechanism to drive the plates; however, a chief argument against convective shear being a major plate-driving force is the amount of time required for the flow pattern to change (Richter, 1973). Directional and rate changes of the plates occur on a much shorter time scale. Artyushkov (1973) argued that the low viscosity of the asthenosphere is not sufficiently substantial to produce enough shear stress on the base of the plates to drive them, provided convection currents exist in the mantle.

A driving drag model was proposed in which forces proportional to the absolute angular velocity of the plate, $0.247^\circ/\text{m.y.}$ (Minster and Jordan, 1978) were applied in a direction counterclockwise about an absolute pole of rotation at -58.3° N., -40.7° E. The absolute motion parameters were obtained from the hot-spot reference frame. A linear

drag law was used to obtain a first-order estimate for these drag forces. The driving drag forces, F_{dd} , are proportional to and act in the same direction as the absolute velocity of the plate such that:

$$F_{dd} = c V_{abs} = c W_{abs} \times r \quad (5-6)$$

where: c = an arbitrary constant determined such that a plate velocity of 1 cm/yr produces a shear stress of 0.1 MPa

V_{abs} = is the absolute velocity at any point on the plate with radius r

W_{abs} = absolute rotation pole for the plate determined from the torque pole of the nondrag forces.

Resistive Drag

The North American plate is assumed for modeling to be moving at a constant velocity; thus it is not accelerating. Ridge forces driving the plate from its eastern boundary would supply a substantial torque on the plate. This torque must be balanced for the plate to be in mechanical equilibrium. Transform forces and normal forces supplied from adjacent plates may provide some of this balancing resistance to the ridge force; however, this resistance may not be great enough or be supplied in the appropriate directions to completely balance the ridge torque. Therefore, shear stress on the base of the plate may be appealed to as a free parameter balancing force to this net torque. The resistance drag forces are proportional but opposite in sign to an absolute velocity defined for the plate due to the net torque acting on the plate from other forces. The pole of rotation about which these

drag forces are applied is a function of the net torque pole of the other tectonic forces acting on the plate. The same linear drag law, equation (5-6), was used for resistive drag as for driving drag except that the resistive forces are antiparallel to the V_{abs} vectors. Shear tractions equivalent to the calculated drag force acting on a unit area were applied at all node points.

Variable Drag

The asthenosphere underlying continental lithosphere is more viscous than oceanic asthenosphere (Artyushkov, 1973). Therefore, the shear tractions on the base of the continental lithosphere should be greater than those for oceanic lithosphere. Variable drag models in which greater shear tractions along the base of continental lithosphere are assumed may illustrate the effect of this variable viscosity. Drag forces may also vary within the continental and oceanic asthenospheres. For simplicity and lack of data to provide accurate estimations of these differences, only constant drag forces were used in this modeling scheme.

CHAPTER 6

MODELING RESULTS

Numerous tectonic force models were tested to analyze the effects of different loading schemes on North American intraplate stresses. Models are classified according to the boundary and internal force types applied to the plate. The classification scheme used to specify model type is given in Table 1. A description of the models and results will be discussed below. Table 2 is a list of torque and rotation rate poles and magnitudes for each force model.

Ridge Models

Ridge forces may be one of the most significant tectonic forces acting on the North American plate. They are also the best understood forces in terms of magnitude and direction. In initial models, the effects of these forces on the intraplate stress regime were analyzed.

Line Ridge Model

In the line ridge model, line ridge forces were applied along the length of the ridge (Figure 5) and the western boundary of the plate (24 nodes) was pinned from motion in the latitudinal and longitudinal directions. The plate had a constant thickness of 5×10^4 m. Pinning the western boundary is a simplistic means of constraining the plate so that it will deform internally and not accelerate. It is equivalent to assuming that there are forces acting on the North American plate from

Table 1. Description of force models

Model	Force Parameters ^a									Figure
	F _{LR}	F _{GR}	F _{CR}	F _P	F _S	F _N	F _T	F _{RD}	F _{DD}	
LR	1	0	0	0	0	0	0	0	0	5
DR1	0	1	0	0	0	0	0	0	0	6a
DR2	0	0	1	0	0	0	0	0	0	6b
DRD1	0	1	0	0	0	0	0	1	0	16
DRD2	0	0	1	0	0	0	0	1	0	17
DRD3	0	1	0	0	0	0	0	1	0	18
DD	0	0	0	0	0	0	0	0	1	19
DP	0	1	0	1	0	0	0	1	0	20
DPS	0	1	0	1	1	0	0	1	0	21
DPSN	0	1	0	1	1	1	0	1	0	22
TD	0	0	0	0	0	0	1	1	0	25
BT	0	1	0	1	1	1	1	1	0	24

a. Magnitude for F_{LR} is 3×10^{12} N/m, which is equivalent to a stress of 60 MPa across a 5×10^4 -m-thick plate.

Magnitudes for F_P , F_S , and F_N are 5×10^4 N/m, which is equivalent to a stress of 5 MPa across a 1×10^5 -m-thick plate.

Magnitudes for F_{DR} are given in Table 2.

Magnitude for F_{DD} produces 0.1 MPa shear stress for an absolute plate velocity of 1.0 cm/yr.

Table. 2. Torque parameters for force models

Model	Nondrag Torque			Balancing Drag ^a			Figure
	Magnitude N·m	Latitude degrees	Longitude degrees	Rate °/yr	Latitude degrees	Longitude degrees	
LR	9.03×10^{25}	33.13 S.	41.07 W.	---	---	---	5
DR1	5.40	51.25 S.	57.20 W.	---	---	---	6a
DR2	4.23	57.95 S.	66.16 W.	---	---	---	6b
DRD1	5.40	51.25 S.	57.20 W.	2.73×10^{-7}	77.84 S.	3.07 W.	16
DRD2	4.23	57.95 S.	66.16 W.	2.43	81.93 S.	33.07 W.	17
DRD3	5.84	48.14 S.	58.96 W.	2.7	75.66 S.	20.22 W.	18
DD	2.72	38.48 S.	53.99 W.	1.0	58.31 N. ^b	40.67 W.	19
DP	6.28	73.42 S.	109.46 W.	4.86	74.68 N.	98.17 E.	20
DPS	3.95	60.92 S.	156.56 W.	2.95	69.91 S.	120.96 E.	21
DPSN	5.19	33.02 S.	172.86 W.	2.77	56.95 S.	147.07 E.	22
TD	4.87	8.89 N.	13.57 W.	2.02	32.99 S.	34.54 E.	23
BT	2.68	50.48 S.	77.93 W.	1.24	81.33 S.	47.62 W.	25

a. Rate depends on choice of c in equation (5-6), but pole located is independent of c as long as c is constant over the plate.

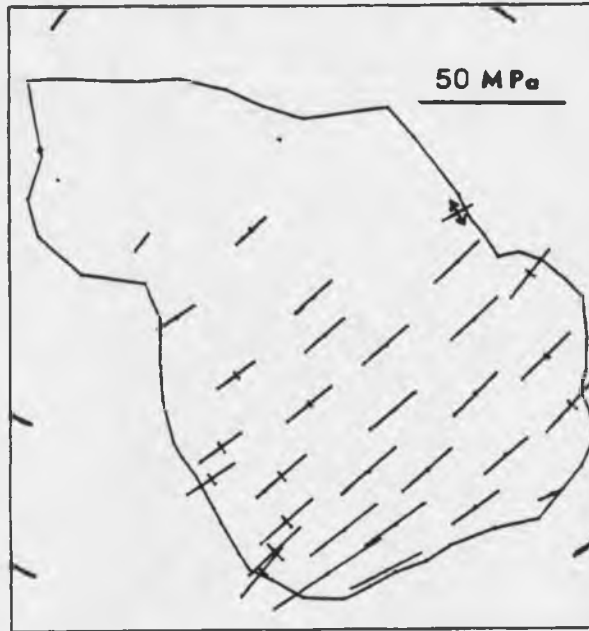
b. Absolute rotation pole from Minster and Jordan (1978).

the Pacific plate that keep the boundary nodes fixed. This is not a realistic model from which to obtain accurate stress magnitudes, but resulting stress orientations are in approximate agreement with the observed stress trends in the Mid-Continent stress province. The resulting stresses from this model are shown in Figure 15.

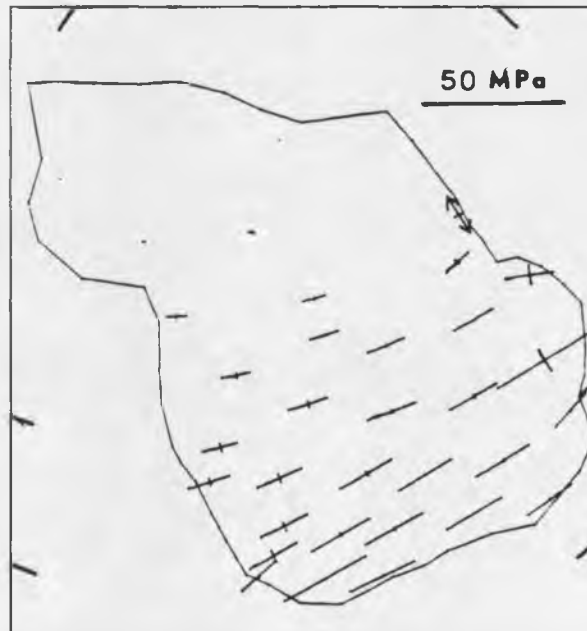
Coarse-grid Distributed Ridge Model

Distributed ridge forces were applied to the plate by using both the gravitational sliding and cooling half-space formulations. These forces are shown in Figure 6. As discovered in the ridge-force test case discussed in Chapter 5, the gravitational sliding forces increase at a more rapid rate near the ridge than cooling half-space forces. Because the amount of oceanic lithosphere for the North American plate away from the ridge decreases northward, so does the cumulative distributed ridge force. In fact, the amount of oceanic lithosphere normal to the ridge above lat 50° N. is so small that ridge forces derived from the cooling half-space formulation are essentially nonexistent. Also, the magnitudes of cooling half-space forces may not be approximated very accurately for elements in which $(\text{area})^{\frac{1}{2}}$ is not a good approximation for l_{\perp} . The net force directions for both ridge-force models are approximately parallel to the increasing-age gradients for the oceanic lithosphere.

For the coarse grid, nodes above 60° N. were spaced so far apart that ridge forces near Greenland and the North Pole actually pointed toward the ridge. For these elements, one node was located on the ridge, whereas the next node was at a higher elevation because it



a. Force model LR



b. Force model DR1

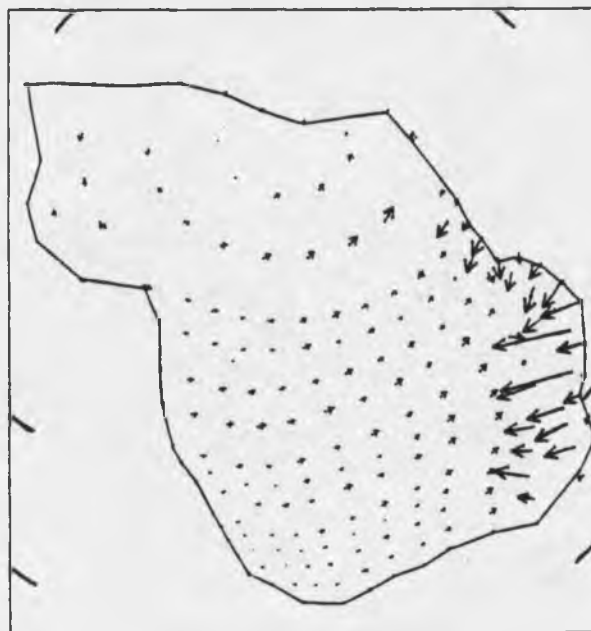
Figure 15. Resulting stresses from ridge force models

was located near Greenland or on the continental shelf of North America. Thus, ridge forces for these elements were eliminated from the coarse-grid tests.

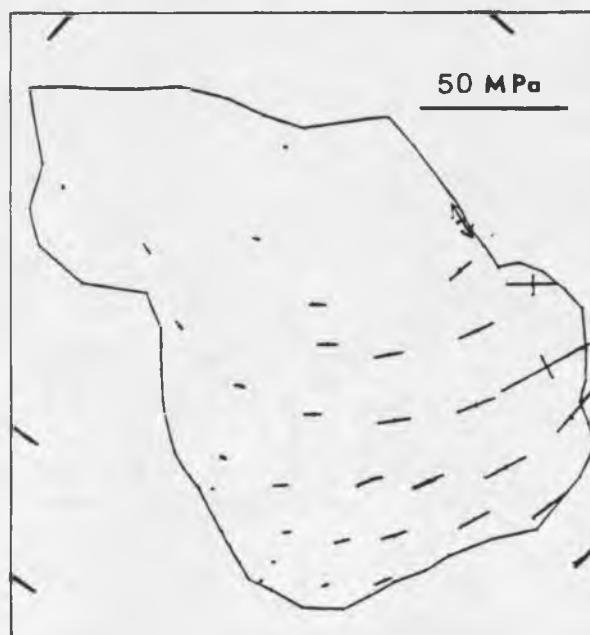
For both of these models, the western boundary was pinned as in the line ridge model. The only substantial difference in the stress results from the line ridge model, LR (Table 1), and the distributed-ridge models, DR1 and DR2 (Table 1), occurs near the ridge. Also, the general trend of the line ridge stresses in the Mid-Continent stress province is N. 70° E. for model LR and N. 80° E. for model DR1 (Figure 15). A comparison of the torque poles and magnitudes for these two models can be made by referring to Table 2.

Additional distributed ridge models, DRD1 and DRD2 (Table 1) with different boundary conditions were also tested. In these models, three degrees of freedom were constrained. Node 184, near the North Pole at 80° N., 110° W., was constrained in the latitudinal and longitudinal directions, and node 7, along the southern plate boundary at 19° N., 183° W., was constrained in the longitudinal direction to prevent the plate from spinning about node 184. Resistive drag forces were called upon to balance the torque due to ridge forces. A consequence of the large element size above 60° N. is the apparent large magnitude of the drag forces. This is an artifact of elemental area, because drag forces per unit area are constant.

The gravitational sliding distributed ridge forces and balancing drag forces for model DRD1 are shown in Figure 16. The stresses from this model are also shown in Figure 16. Likewise, the cooling half-space forces and stresses of model DRD2 are shown in Figure 17. The

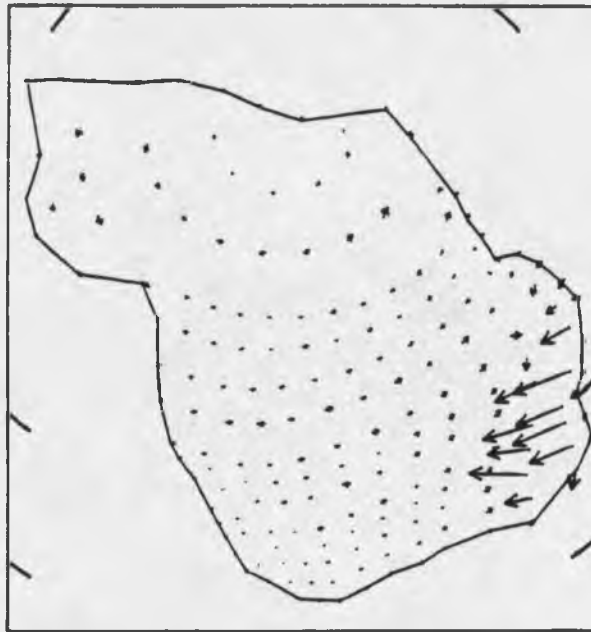


a. Forces

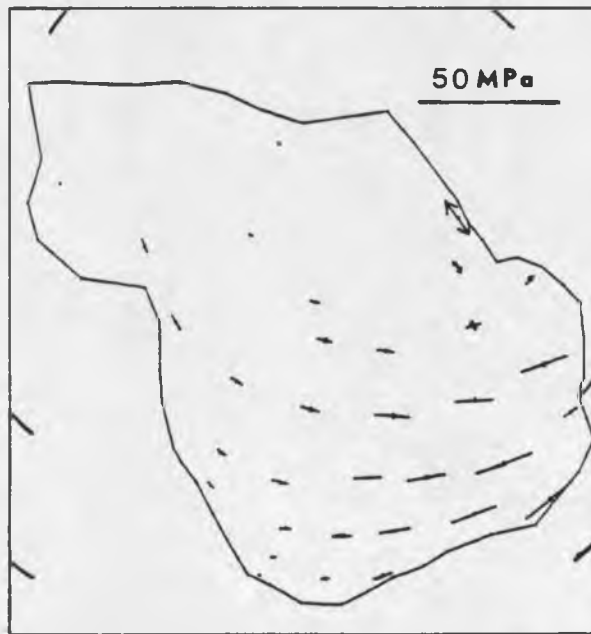


b. Stresses

Figure 16. Force model DRD1 and resulting stresses



a. Forces



b. Stresses

Figure 17. Force model DRD2 and resulting stresses

total torque on the plate due to forces in model DRD1 is 5.4×10^{25} N·m (N·m = newtons times meters), which is slightly larger than the value for the total torque, 4.23×10^{25} N·m due to forces in model DRD2.

Slight differences in stress magnitudes and orientations were observed near the ridge. A few differences should be noted in comparing the stresses from both of these distributed ridge models with drag to those from model DR without drag (Table 1). The principal stress orientations away from the ridge remain relatively constant for the DR model (Figures 15). However, for the DRD models (Figures 16 and 17), the stress orientations from the mid-plate regions westward vary from east-west in the southern portion to east-southeast in the northern portion. The reason for this change in stress trends away from the ridge is obviously related to the drag forces in the model. Ridge forces appear to control the stress trends in the eastern portion of the plate; however, in the west, drag forces appear to dominate the effect of ridge forces and hence stresses in this region are approximately subparallel to the drag forces. The dependence of stresses on drag forces could be reduced by incorporating other torque-balancing forces in the modeling scheme. In all subsequent models that include other plate boundary forces, however, resistive drag forces were called upon to balance net torques acting on the plate.

Fine-grid Distributed Ridge Model

Because of the inherent problems associated with coarse-grid modeling such as the limited resolution of stresses and the inability to accurately model forces that vary spatially in or along the boundaries of

the plate, a finer grid was constructed. All initial models were conducted using the coarse grid, which allowed for economical tests of each model. The gravitational sliding distributed ridge forces calculated using the fine grid are shown in Figure 18. Forces above lat 60° N. reveal the topographic effects of Iceland and Greenland. The resultant stresses from this model, DRD3 (Table 1), are shown in Figure 18. The only significant differences in the stresses of the coarse-grid model DRD1 and the fine-grid model DRD3 are the presence of stresses in the northernmost portion of the plate for DRD3 and a slightly north of east orientation for mid-latitude DRD3 stresses near the ridge. Maximum principal stress orientations in the Mid-Continent stress province are oriented approximately east-west, an orientation that differs by approximately 23 degrees in a clockwise direction from observed orientations. The forces from model DRD3 result in a slightly larger nondrag torque magnitude of 5.84×10^{25} N·m than the 4.5×10^{25} N·m magnitude for model DRD1. The torque poles (Table 2) for both of these models are however very similar.

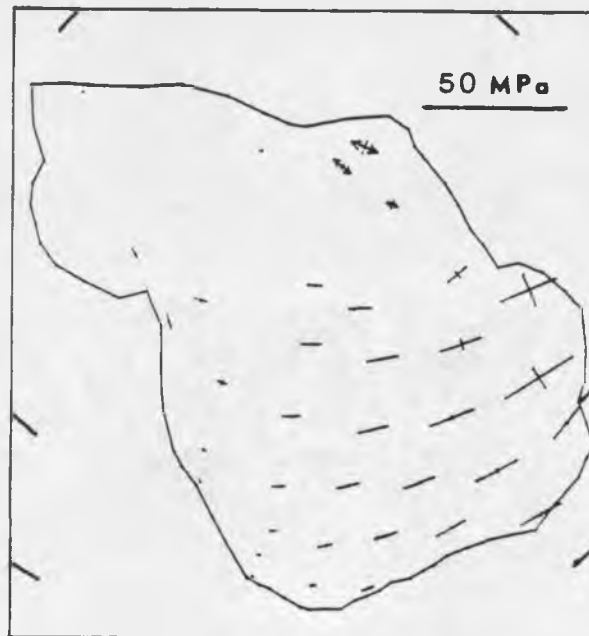
All subsequent modeling results are presented from fine-grid models; all models that incorporate ridge forces have ridge forces according to the gravitational sliding formulation.

Driving-drag Model

In addition to the pinned ridge-force models, a driving-drag model, DD (Table 1) was found to also fit the dominant east-northeast Mid-Continent stress trend. In this model the North American plate is driven by viscous drag forces that act in the direction of absolute plate



a. Forces



b. Stresses

Figure 18. Force model DRD3 and resulting stresses

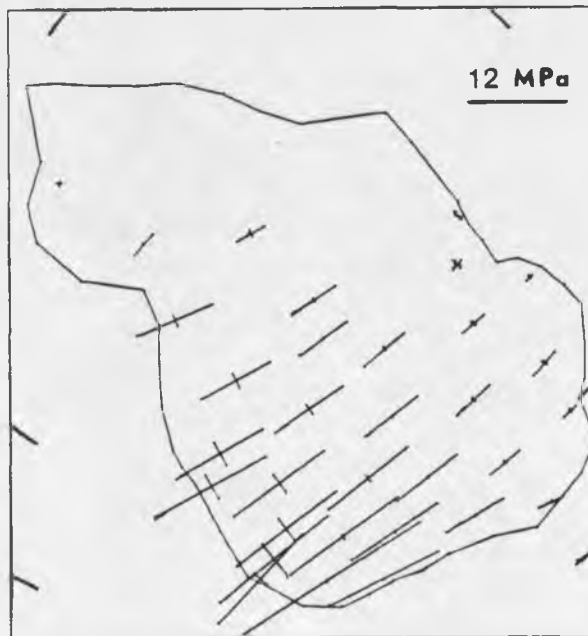
motion at an absolute rotation rate of $0.247^\circ/\text{m.y.}$ (Minster and Jordan, 1978). The western plate boundary was pinned from motion. These drag forces are shown on Figure 19a. These forces act in approximately the same direction as the ridge forces; therefore, the orientations of the stresses (Figure 19b) are similar to those of the stresses from the LR and DR models. The major difference between model DRD and model DD is that the DD stresses increase from null values near the ridge to very large values in the western portion of the plate in contrast to stresses from the DRD1 model, which decrease in magnitude from east to west. Hence, if driving drag forces had been used instead of ridge forces to fit the east-northeast compressive stress trends in the Mid-Continent stress province, models that included all other boundary forces would have resulted in large stresses in the western portion of the plate and relatively insignificant stresses in the eastern portion. Also, resistive drag forces could not be used as a free balancing force to assure mechanical equilibrium for the plate.

Pacific-Boundary Model

In model DP (Table 1), forces were applied along the San Andreas and Aleutian segments of the Pacific-North American plate boundary. These forces are described in detail in Chapter 5. Various magnitudes for these boundary forces were tested. A shear stress of 5 MPa applied across the $1 \times 10^5\text{-m}$ plate thickness along the San Andreas transform was found to be sufficient for the boundary forces to control stress trends in the San Andreas stress province. It is unlikely that most of this shear stress along the fault is supported equally across the



a. Forces



b. Stresses

Figure 19. Force model DD and resulting stresses

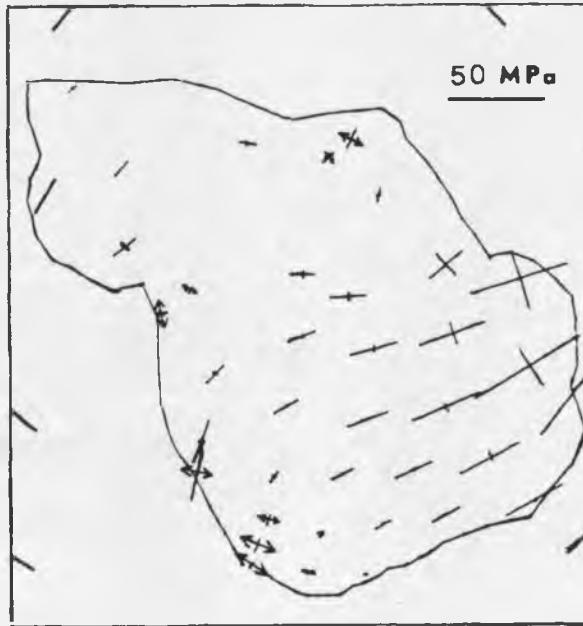
entire 1×10^5 -m thickness of the plate. It is more likely that most of the stress in the lithosphere is concentrated in the upper 10 km; therefore, stress magnitudes as large as 50 MPa or more could exist near the surface of the plate along the San Andreas transform. A few hundred kilometers away from the fault, however, unless decoupling exists in the crust, actual partitioning of the shear tractions over depth along the San Andreas transform is probably averaged out so that these forces could appear as if they are equivalent to 5 MPa throughout the entire 1×10^5 -m plate thickness.

It was only in this province and in the southern Basin and Range stress province that stresses appear to be affected by these transform forces. The forces applied along the Aleutian arc complex were scaled such that an average compressive stress magnitude of 5 MPa for the a 1×10^5 -m plate thickness resulted near the trench. These Pacific boundary forces along with the ridge and resistive drag forces are shown in Figure 20.

Landward from the Aleutians, the calculated maximum principal stresses trend approximately perpendicular to the plate boundary and agree with observed stress states, although there is now an indication that stresses in Alaska may be more complex than can be explained by model DP (Cook and others, 1984). (See Table 2). In the San Andreas stress province, principal stress trends fit the data quite accurately. Maximum principal stresses are oriented approximately north-south to north-northeast. East-west deviatoric tensional stresses in the San Andreas stress province become the least principal stresses in the Southern Basin and Range stress province; when shear stress



a. Forces



b. Stresses

Figure 20. Force model DP and resulting stresses

magnitudes greater than 5 MPa are applied along the San Andreas transform, large north-south principal compressive stresses increase in the northeast Pacific stress province. For shear stresses as large as 10 MPa, stress states in the entire western region of the plate appear to be most greatly affected by the transform forces. It is unlikely that shear stresses along the San Andreas transform could be transmitted west of the thin, soft Basin and Range stress province (Richardson, 1974); therefore, models for which shear tractions applied along the San Andreas transform are greater than 6 MPa averaged over the 1×10^5 -m-thick plate result in unrealistic stress magnitudes and orientations east of the Basin and Range stress province.

The magnitudes of balancing drag forces for model DP are even larger than those in model DRD 3 (Table 2). This result is due to the effect of ridge and Pacific forces both acting in directions that cause the plate to rotate clockwise about the torque pole. Additional forces along the southern boundary would act to oppose this rotation and partially balance the net torque due to these other forces.

Southern Boundary Model

In addition to tectonic forces acting along the eastern and Pacific boundaries, forces due to plate interactions along the southern boundary of the North American plate should also be considered in the modeling scheme. Compressional forces related to the subduction of the Cocos plate beneath Mexico and shear tractions along the Caribbean transform were discussed in Chapter 5 and shown in Figs. 14. The magnitudes of these forces are unknown and poorly constrained by

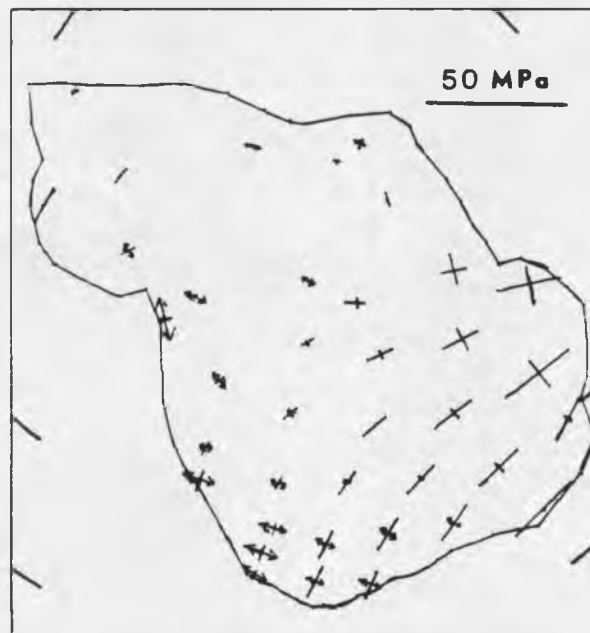
inferred stress magnitudes. Therefore, a consistent scaling factor was used for southern and western boundary forces. The model, DPS (Table 1), which incorporates ridges, subduction-related, transform, and resistive drag forces, is illustrated in Figure 21a. Resulting stresses from this model are shown in Figure 21b. The magnitudes of the nondrag torque and the balancing drag rate are substantially reduced from those of DP model (Table 2).

The maximum principal stresses appear to have reasonably acceptable orientations. In the Mid-Continent stress province, these stress orientations trend approximately N. 70° E. It should be noted that very little data exists in this southern region to constrain the results. Normal to these maximum principal stresses, however, deviatoric tensional stresses appear to be too large and too widespread as evidence by the large south-west deviatoric tensional stresses in the San Andreas stress province, which are larger than the north-south maximum compressive principal stresses. These tensional features appear to be the direct result of the San Andreas and Caribbean shear tractions essentially pulling the plate apart about its southwest corner. The necessity of forces acting normal to the transform boundaries was realized from observing this effect.

Forces normal to both transform boundaries were applied at each node along the transforms. The normal forces were initially given the same magnitudes as their corresponding transform forces. The resulting transform forces are equal to the vector sum of the normal



a. Forces



b. Stresses

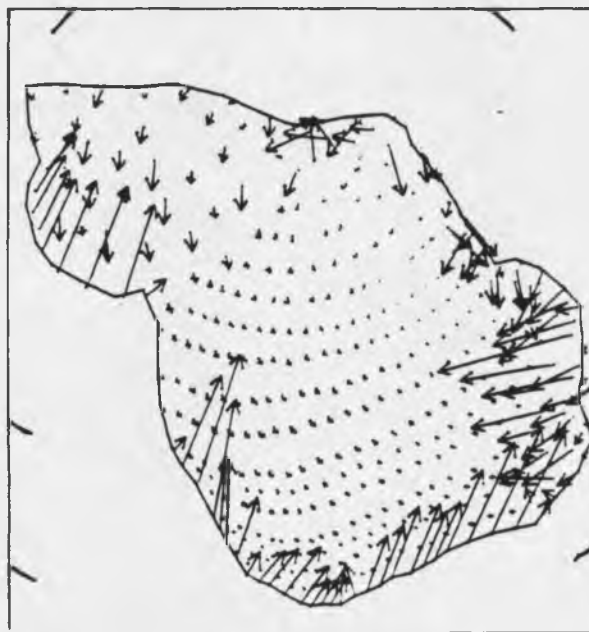
Figure 21. Force model DPS and resulting stresses

forces and the shear tractions. They are shown in Figure 22 along with the other forces used in this model, DPSN (Table 1).

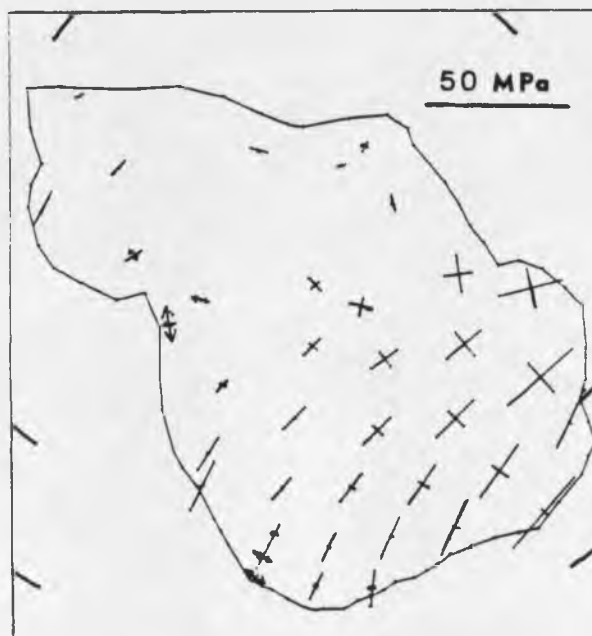
To this end, this model seems to be the most realistic, and it produces stresses that best fit the data (Figure 22). Calculated stresses throughout the entire Mid-Continent stress province consistently fit the data. Predicted stresses inward from all boundaries are also in agreement with observed stresses. Possibly the only regions in which stress orientations are not in agreement with the observed stresses include those provinces for which stresses are believed to be due to localized effects. These regions include the Atlantic Coast stress province in the east and the Basin and Range, Colorado Plateau, and Southern Great Plains stress provinces. Attempts to fit the stress data in these regions were done by incorporating forces due to continental topography into the model scheme.

Continental Topography Model

Topographic forces based on the density moment formulation discussed in Chapter 5 were incorporated into the modeling scheme in hope of better fitting stress trends in the western and continental shelf portions of the North American plate. These topographic forces are shown in Figure 12. A few patterns should be noted. One is the consistent downdip alignment of forces on the continental shelves. Forces emanating from the Basin and Range stress province are generally pointing toward the east, consistent with the idea that the Basin and Range acts like a mid-ocean ridge due to the gravitational potential associated with its elevation. It should also be noted that the apparent



a. Forces



b. Stresses

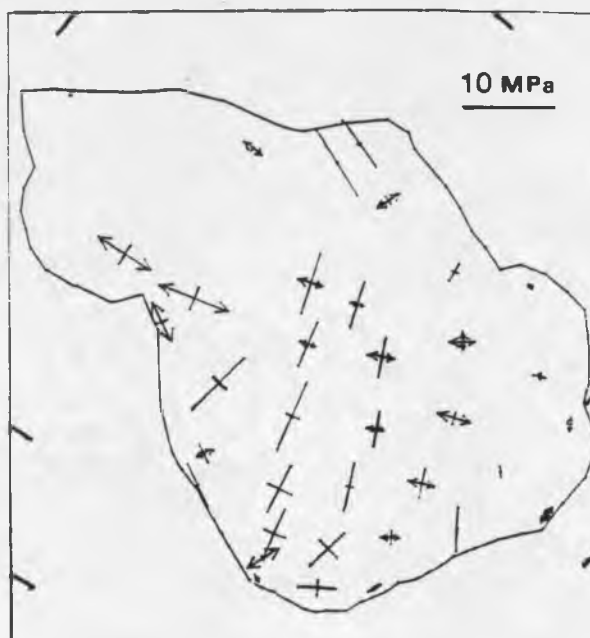
Figure 22. Force model DPSN and resulting stresses

magnitudes of forces near the North Pole are large because of the large elemental areas. In general, forces appear to agree with the results obtained in the topographic test case in which forces point away from higher elevations for regions of constant crustal thickness and point toward thicker crust for regions of constant topography.

Model TD (Table 1) contains only continental topography forces and balancing drag forces (Figure 23a). The resultant stresses (Figure 23b) do not appear to fit the observed data well. This poor fit to the data could possibly be explained by the balancing drag forces controlling the stress trends in the continental portion of the plate. Another explanation could be that continental topography does not affect the intraplate stress regime or that topography only affects stress trends on a local basis. Another possible explanation may be that a combination of tectonic and topography forces is responsible for the nature of the intraplate stresses. These forces were added to the DPSN model to obtain a more realistic approximation of the tectonic and intraplate forces acting on the North American plate. Stresses from this model, BT (Table 1) are shown in Figure 24. These results are not significantly different from those from the DSPN model. The force plot (Figure 25) reveals the significantly smaller magnitude of the continental topography forces as compared to the other boundary forces. As discussed earlier, the density moment formulation used to model the topography forces is based on poorly known subsurface density structures in the lithosphere. This model produces the smallest nondrag torque on the plate of 2.68×10^{25} N·m and a relatively small balancing drag rate of 1.24×10^7 °/yr.



a. Forces



b. Stresses

Figure 23. Force model TD and resulting stresses

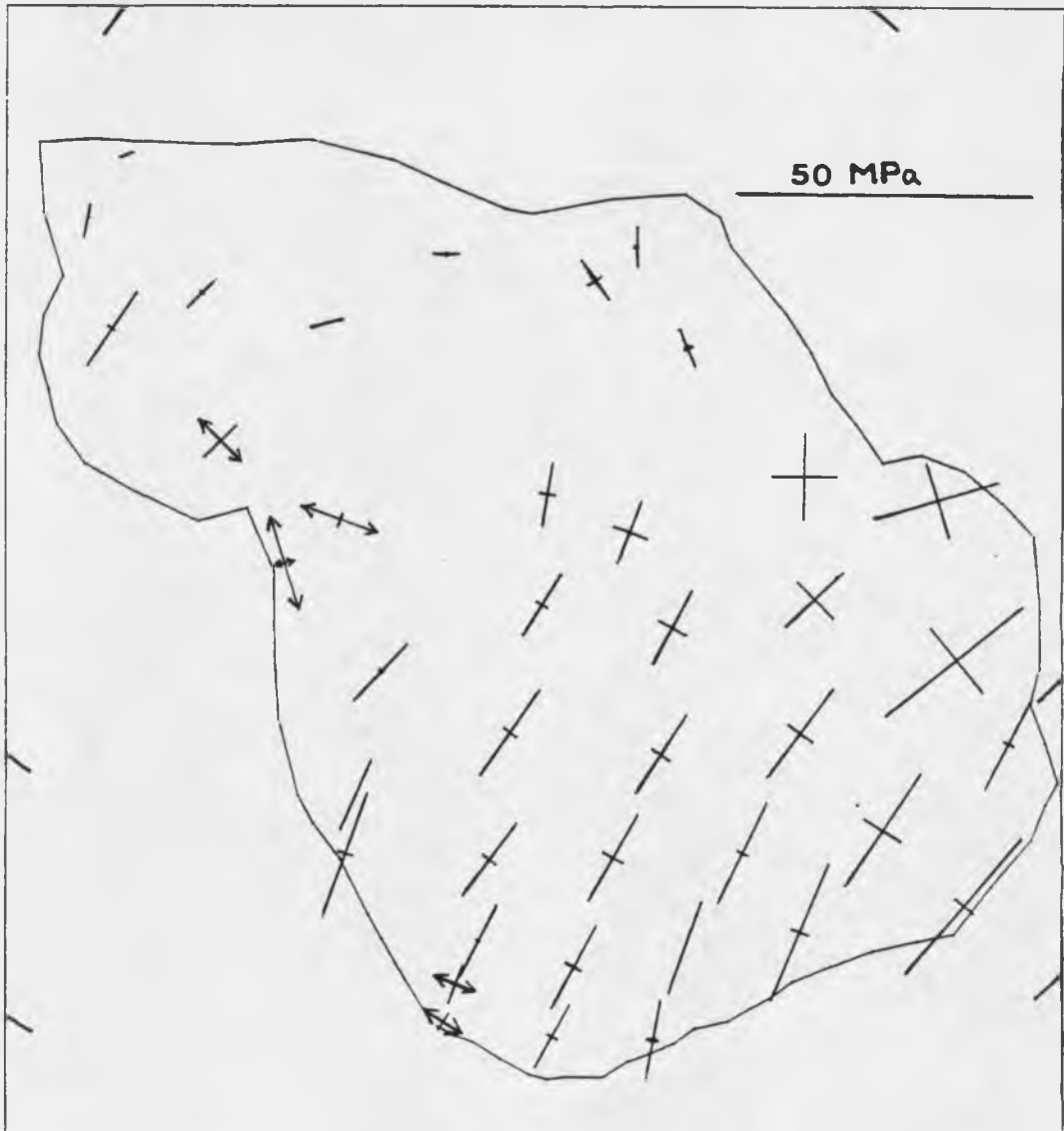


Figure 24. Resulting stresses from force model BT

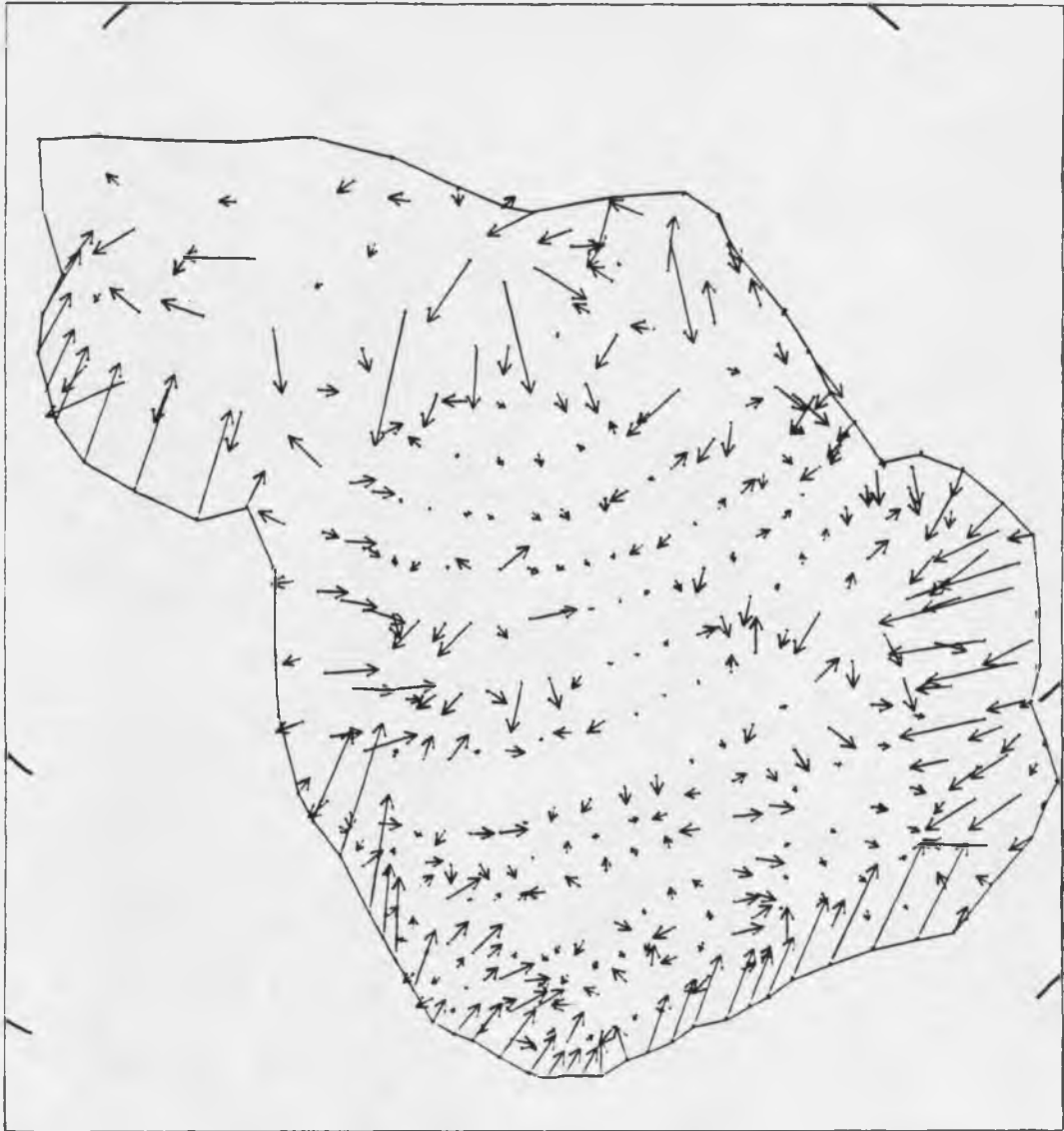


Figure 25. Model BT forces

CHAPTER 7

DISCUSSION AND CONCLUSIONS

It had been the purpose of this thesis to model features of the intraplate stress field for North America in terms of the potential plate-driving and resisting forces that act along the edge and on the base of the plate. An attempt was also made to investigate the possible effects of intraplate forces related to continental topography on localized stress patterns.

Although the details of the driving mechanism of plate tectonics are uncertain, some form of thermal convection due to excess heat energy in the earth is probably responsible for motion and deformation of the plates. Ridge forces are one such force that may be directly related to the upwelling of hot mantle material at plate divergence zones. Drag forces acting on the base of the lithosphere are another type of force that is a direct effect of mantle flow on the base of the lithosphere.

These tectonic forces affect not only the interplate stress regime but the intraplate stress field as well. Intraplate stresses may also be related to residual effects of past activity along transform and subduction boundaries. The complexity of the western stress field of North America can be attributed to present plate interactions along the Pacific boundary (Zoback and Zoback, 1980) and to residual effects of past subduction of the plate along its western edge (Atwater, 1970).

In this modeling scheme, only boundary and basal forces related to present plate tectonics are modeled for the North American plate. Internal plate mechanisms related to the varying rheologic and geologic properties of different physiographic provinces also affect intraplate stresses.

Although attempts to model intraplate stresses in the western portion of the plate are made in this modeling scheme by including topography-related forces, not all of the factors which contribute to intraplate deformation have been modeled such as rheologic changes associated with the anomalously hot upper mantle material caused by cessation of subduction in the west (Zoback and Zoback, 1980). Other dynamic effects related to initiation of transform faulting in the west and second-order effects related to active kinematics for surrounding regions of the Colorado Plateau and Great Plains areas seem to complicate the stresses in these areas (Zoback and Zoback, 1980) and were not considered in this modeling scheme.

The source of stress causing a rotation of principal stresses along the Atlantic Coast north of Virginia and south of Maine is also uncertain. The possible orientation in this area of principal stresses approximately normal to the inferred stresses of the mid-continental and oceanic regions could be related to localized effects superimposed on the effect of ridge forces that are believed to possibly control the orientations of stresses in surrounding regions. Sediment-loading phenomena and lateral density changes normal to the continental margin may account for some of these inferred orientations normal to the margin. Stress orientations may also be related to the pattern of gravity

anomalies in the region, which can be explained by surface and subsurface loads along the length of the Appalachian fold belt (Karner and Watts, 1983). These loads are probably related to fold and thrust blocks; therefore, different tectonic structures in the northern and southern Appalachians may account for the different stress orientations in these two regions of the Atlantic coastal stress province. Lithospheric flexure and lateral density contrasts associated with a continental margin predict extensional features for shelf regions (Bott and Dean, 1982; Zoback and Zoback, 1980). However, the inferred stresses for the Atlantic coastal margin are compressional.

The extensional tectonics predicted for the continental margin by Bott and Dean among others is the result of oversimplified models that consider only changes in the mechanical properties of the shelf, e.g., lateral density contrasts; the "pushing" effect of the ridge on the shelf is not considered. Modeling the shelf according to a density moment scheme, as shown in this thesis, incorporates the relative effect of density moment changes associated with the shelf superimposed on the effect of the ridge pushing on the shelf. The shelf effect, as modeled with density moments, predicts a decrease in compressive stresses normal to the shelf.

Even though attempts were made to fit local features of the intraplate stress field of North America by modeling lateral density differences within the plate and refining the finite-element grids to increase the detail of the loading schemes and increase resulting stress resolution, many stress features are not resolved and are believed to be due to complex localized past and present processes acting within the

plate. However, modeling of the boundary and basal forces acting on the plate is quite conclusive. An outline of the modeling results is presented and major conclusions that have been drawn concerning the validity and versatility of this modeling scheme will be presented.

1. Distributing ridge forces throughout the entire topographic expression of the oceanic portion of the North America plate is a more realistic and accurate way to approximate forces due to the gravitational potential of the elevated Mid-Atlantic Ridge than the previously used line ridge approximation method of Richardson (1978b). However, the line ridge model was found to be a good first approximation to the distributed ridge models with the exception of the resultant stresses near the ridge. For the line ridge model, the near-ridge stress magnitudes remain almost constant, unlike those for the DRD models, which decreases as the total cumulative force decreases toward the ridge.

2. It was determined that expressions that quantify ridge forces as a function of distance from the ridge could be formulated according to either a cooling half-space phenomenon or according to the gravitational potential associated with the lateral changes in density associated with the cooling sinking lithosphere. Expressions of both types were formulated and found to yield comparable results in both magnitude and direction. However, because the cooling formulation depends on knowledge about the past cooling history of any point along the lithosphere and an approximation has to be used to estimate the length normal to the ridge for any element, the gravitational sliding formulation was chosen for use in all subsequent models that had ridge forces. All ridge models approximately fit the dominant east-northeast

mid-continental compressive stress trend. However, there were significant differences in those models in which resistive drag forces kept the plate in mechanical equilibrium. Models in which drag forces were applied seemed to indicate that drag forces alone were probably not a viable balancing force because they tended to control the intraplate stress trends in the west as much as, if not more than, the ridge forces.

3. Even though mid-plate stresses were fit with a driving-drag model, other shortcomings in this model left the ridge models as more realistic models of the tectonic processes acting on the North American plate.

4. The only significant difference between coarse- and fine-grid modeling results is that ridge forces were included above lat 60° N. for fine-grid models and not for coarse-grid models. Thus, the stress states in this northern region were modeled more accurately in the fine-grid models. Intraplate topographic and crustal thickness features were modeled more accurately with the smaller element sizes. The major conclusions drawn from both grid models are the same.

5. Addition of Pacific boundary forces along the San Andreas transform and Aleutian arc complex to the modeling scheme resulted in good fits to the stress data in these western regions. The magnitudes of these forces are only weakly constrained, but magnitudes that yielded stresses on the order of 5 MPa averaged over the 1×10^5 -m-thick lithosphere resulted in the most acceptable stress results.

6. When normal forces due to the Cocos plate and shear forces due to the Caribbean plate were added, less resistive drag was required to

balance ridge forces. However, the incorporation of these forces resulted in large extensional stresses in the southwestern portion of the North American plate.

7. Normal forces across transform boundaries were found to be essential to obtain reasonably accurate intraplate stress orientations.

8. The density moment formulation based on continental topography and crustal thicknesses was found to be very dependent on assumptions made about the density structure in the lithosphere and the compensation mechanism characteristic of certain regions of the plate. Evidence based on geoid anomalies agreed with moment magnitudes calculated for the continent. The resultant topography forces were found to be almost insignificant relative to the other boundary forces. The topography forces alone did not seem to produce stresses that accurately matched those in the western and coastal regions of the North American plate.

REFERENCES

- Artyushkov, E. V., 1973, Stresses in the lithosphere caused by crustal thickness inhomogeneities: *J. Geophys. Res.*, v. 78, p. 7875-7708.
- Atwater, T., 1970, Implications of plate tectonics for the Cenozoic tectonic evolution of western North America, in Cox, A., ed., *Plate tectonics and geomagnetic reversals*: San Francisco, W. H. Freeman and Co.
- Ball, M. M., and Harrison, C. G. A., 1980, Crustal plates in the central Atlantic Ocean: *Science*, v. 167, p. 1128-1129.
- Bathe, K. J., and Wilson, E. L., 1976, *Numerical methods in finite element analysis*: Englewood Cliffs, New Jersey, Prentice-Hall.
- Blake, M. C., Jr., Campbell, R. H., Dibblee, T. W., Jr., Howell, D. G., Nielsen, T. H., Normark, W. R., Vedder, J. C., and Silver, E. A., 1978, Neogene basin formation in relation to plate-tectonic evolution of the San Andreas fault system, California: *Amer. Assoc. Petrol. Geol. Bull.*, v. 62, p. 344-372.
- Bott, M. H. P., and Dean, D. S., 1972, Stress systems at young continental margins: *Nature*, v. 235, p. 23-25.
- Brune, J. N., Henyey, T. L., and Roy, R. F., 1969, Heat flow, stress, and rate of slip along the San Andreas fault, California: *J. Geophys. Res.*, v. 74, p. 3821-3827.
- Chael, E. P., and Stewart, G. S., 1982, Recent large earthquakes along the Middle American trench and their applications for the subduction process: *J. Geophys. Res.*, v. 87, p. 329-338.
- Chase, C. G., 1984, Plate kinematics, the Americas, East Africa, and the rest of the world: *Earth and Planetary Science Letters*, v. 37, p. 355-368.
- Chase, C. G., 1984, Personal communication: Assistant professor of Geosciences, University of Arizona, Tucson.
- Fleitout, L., and Froidevaux, C., 1982, Tectonics and topography for a lithosphere containing density heterogeneities: *Tectonics*, v. 1, p. 21-38.
- Fleitout, L., and Froidevaux, C., 1983, Tectonic stress in the lithosphere: *Tectonics*, v. 2, p. 315-324.

- Fordjor, C. K., Bell, J. S., and Gough, D. T., 1983, Breakouts in Alberta and stress in the North American plate: *Canadian Jour. Earth Sci.*, v. 20, p. 1445-1455.
- Forsyth, D. W., and Uyeda, S., 1975, On the relative importance of driving forces of plate motion: *Geophys., Jour. Roy. Astron. Soc. [London]*, v. 43, p. 163-200.
- Frank, F. C., 1972, Plate tectonics, the analogy with glacier flow and isostasy, in *Flow and fracture of rocks*: Washington, D. C., American Geophysical Union, *Geophys. Mon. Ser.*, v. 16, p. 285-292.
- Frohlich, C., 1982, Seismicity of the central Gulf of Mexico: *Geology*, v. 10, p. 103-106.
- Funnell, B. M., and Smith, A. G., 1968, Opening of the Atlantic Ocean: *Nature*, v. 219, p. 1328-1333.
- Gough, D. I., Fordjor, C. K., and Bell, J. S., 1963, A stress province boundary and tractions on the North American plate: *Nature*, v. 305, p. 619-621.
- Hager, B. H., and O'Connell, R. J., 1981, A simple global model of plate dynamics and mantle connection: *J. Geophys. Res.*, v. 86, p. 4843-4867.
- Haimson, B. C., 1977, Crustal stress in the continental United States as derived from hydrofracturing tests, in Heacock, J. C., ed., *The Earth's crust*: Washington, D. C., American Geophysical Union, *Geophys. Mon. Ser.*, v. 20, p. 576-592.
- Haxby, W. F., and Turcotte, D. L., 1978, On isostatic geoid anomalies: *J. Geophys. Res.*, v. 83, p. 5473-5478.
- Hess, H. H., 1972, History of ocean basins in plate tectonics and geomagnetic reversals, in Cox, A., ed., *Plate tectonics and geomagnetic reversals*: San Francisco, W. H. Freeman and Co., p.
- Hickman, S. H., Healy, J. H., and Zoback, n.d., In-situ stress, natural fracture distribution, and borehole elongation in the Auburn geothermal well, Auburn, New York: *J. Geophys. Res.*, in press, 1984.
- Irons, B. M., 1970, A frontal solution program for finite element analysis: *Intern. Jour. Num. Method Eng.*, v. 2, p. 5-32.
- Jacoby, W. R., 1970, Instability in the upper mantle and global plate movements: *J. Geophys. Res.*, v. 75, p. 5671-5680.

- Karner, G. D., and Watts, A. B., 1983, Gravity anomalies and flexure of the lithosphere at mountain ranges: *J. Geophys. Res.*, v. 88, p. 10449-10477.
- Lackenbruch, A. H., and Sass, J. H., 1980, Heat flow and energetics of the San Andreas fault zones: *J. Geophys. Res.*, v. 85, p. 6185-6222.
- Lister, C. R. B., 1975, Gravitational drive on oceanic plates caused by thermal contraction: *Nature*, v. 257, p. 663-665.
- Minster, J. B., and Jordan, T. H., 1978, Present-day plate motions: *J. Geophys. Res.*, v. 83, p. 5331-5354.
- Nakamura, K., Jacob, K. H., and Davies, J. N., 1978, Volcanoes as possible indicators of tectonic stress orientations--Aleutians and Alaska: *Pure Appl. Geophys.*, v. 115, p. 67-112.
- Nakiboglu, S. M., 1982, Hydrostatic theory of the Earth and its implications: *Phys. Earth Planet. Letters.*, v. 25, p. 302-311.
- Newmark, R. L., Zoback, M. D., and Anderson, R. N., 1984, Determination of in situ stress directions in the crust: DSDP hole 597c: *EOS, Trans. Amer. Geophys. Union*, v. 65, p. 219.
- Parsons, B., and Richter, F. M., 1980, A relation between driving force and geoid anomaly associated with the mid-ocean ridges: *Earth Planet. Sci. Letters*, v. 51, p. 445-450.
- Richardson, R. M., 1978a, Finite element modeling of stress in the Nazca plate: driving forces and plate boundary earthquakes: *Tectonophysics*, v. 50, p. 223-248.
- Richardson, R. M., 1978b, Intraplate stress and the driving mechanism for plate tectonics: Unpublished Ph.D. thesis, Massachusetts Institute of Technology, Cambridge.
- Richardson, R. M., 1984, A short discourse on the driving mechanism for plate tectonics with special emphasis on earthquake hazard for the eastern United States: Unpublished paper, Department of Geosciences, University of Arizona, Tucson.
- Richardson, R. M., Solomon, S. C., and Sleep, N. H., 1976, Intraplate stress as an indicator of plate tectonic driving forces: *J. Geophys. Res.*, v. 81, p. 1847-1856.
- Richter, F. M., 1973, Dynamic models for seafloor spreading: *Rev. Geophys. Space Phys.*, v. 11, p. 223-287.

- Sbar, M. L., and Sykes, L. R., 1973, Contemporary compressive stress and seismicity in eastern North American: An example of intraplate tectonics: *Geol. Soc. America Bull.*, v. 84, 1961-1882.
- Soller, D. R., Ray, R. D., and Brown, R. D., 1982, A new global thickness map: *Tectonics*, v. 1, p. 125-149.
- Stauder, W., 1968, Tensional character of earthquake foci beneath the Aleutian trench with relation to sea floor spreading: *J. Geophys. Res.*, v. 73, p. 7693-7701.
- Stewart, J. H., 1977, Basin-range structure in western North America: A review, in Smith, R. B., and Eaton, E. P., eds., *Cenozoic tectonics and regional geophysics of the western Cordillera*: *Geol. Soc. America Memoir* 152, p. 1-31.
- Sykes, L. R., McCann, W. R., and Kafka, A. L., 1982, Motion of Caribbean plate during the last 7 million years and implications for earlier Cenozoic movements: *J. Geophys. Res.*, v. 87, p. 656-676.
- Talwani, P. D., 1982, Internally consistent pattern of seismicity near Charleston, South Carolina: *Geology*, v. 10, p. 664-658.
- Turcotte, D. L., and Schubert, J., 1982, *Geodynamics: Application of continuum geological problems*: New York, Wiley.
- Zienkiewicz, D. C., 1971, *The finite element method in engineering science*: London, McGraw-Hill.
- Zoback, M. D., Healy, J. H., Roller, J. C., Gohn, G. S., and Higgins, B. B., 1978, Normal faulting and in situ stress in the South Carolina coastal plain near Charleston: *Geology*, v. 6, p. 147-152.
- Zoback, M. D., Tsukahara, H., and Hickman, S., 1980, Stress measurements at depth in the vicinity of the San Andreas fault: Implications for the magnitude of shear stress at depth: *J. Geophys. Res.*, v. 85, p. 6157-6173.
- Zoback, M. L., 1984, Personal communication: Reston, Virginia, U.S. Geological Survey.
- Zoback, J. L., Nishenko, S. P., Richardson, R. M., Hasegawa, H. S., and Zoback, M. D., n.d., Mid-plate stress, deformation and seismicity, Chapter C7, in *Decade of North American geology, North Atlantic Volume*: *J. Geophys. Res.*, in preparation [1984].

Zoback, M. L., and Zoback, M. D., 1980, States of stress in the coterminous United States: J. Geophys. Res., v. 85, p. 6113-6156.